



Universiteit  
Leiden  
The Netherlands

## **Heating histories and taphonomy of ancient fireplaces: a multi-proxy case study from the Upper Palaeolithic sequence of Abri Pataud (Les Eyzies-de-Tayac, France)**

Braadbaart, F.; Reidsma, F.H.; Roebroeks, W.; Chiotti, L.; Slon, V.; Meyer, M.; ... ; Marquer, L.

### **Citation**

Braadbaart, F., Reidsma, F. H., Roebroeks, W., Chiotti, L., Slon, V., Meyer, M., ... Marquer, L. (2020). Heating histories and taphonomy of ancient fireplaces: a multi-proxy case study from the Upper Palaeolithic sequence of Abri Pataud (Les Eyzies-de-Tayac, France). *Journal Of Archaeological Science Reports*, 33, 102468. doi:10.1016/j.jasrep.2020.102468

Version: Publisher's Version

License: [Creative Commons CC BY 4.0 license](https://creativecommons.org/licenses/by/4.0/)

Downloaded from: <https://hdl.handle.net/1887/3188479>

**Note:** To cite this publication please use the final published version (if applicable).



ELSEVIER

Contents lists available at ScienceDirect

## Journal of Archaeological Science: Reports

journal homepage: [www.elsevier.com/locate/jasrep](http://www.elsevier.com/locate/jasrep)

# Heating histories and taphonomy of ancient fireplaces: A multi-proxy case study from the Upper Palaeolithic sequence of Abri Pataud (Les Eyzies-de-Tayac, France)



F. Braadbaart<sup>a,b,1</sup>, F.H. Reidsma<sup>a,b</sup>, W. Roebroeks<sup>a,\*</sup>, L. Chiotti<sup>c</sup>, V. Slon<sup>d</sup>, M. Meyer<sup>d</sup>,  
I. Th ery-Parisot<sup>e</sup>, A. van Hoesel<sup>a,f</sup>, K.G.J. Nierop<sup>b</sup>, J. Kaal<sup>g</sup>, B. van Os<sup>f</sup>, L. Marquer<sup>h</sup>

<sup>a</sup> Human Origins, Faculty of Archaeology, Leiden University, Einsteinweg 2 2333CC, Leiden, The Netherlands

<sup>b</sup> Department of Earth Sciences, Faculty of Geosciences, Utrecht University, Princetonlaan 8, 3584 CB Utrecht, The Netherlands

<sup>c</sup> D epartement Homme et Environnement du Mus eum National d'Histoire Naturelle, HNHP UMR du CNRS, Abri Pataud, 20 rue du Moyen- ge, 24620 Les Eyzies-de-Tayac, France

<sup>d</sup> Department of Evolutionary Genetics, Max Planck Institute for Evolutionary Anthropology, Deutscher Platz 6, 04103 Leipzig, Germany

<sup>e</sup> Universit  C te d'Azur, P le Universitaire Saint Jean d'Ang ly, SJA 3 – CEPAM UMR7264 – CNRS – UCA, 24, Avenue des Diables Bleus, 06300 Nice, France

<sup>f</sup> Cultural Heritage Agency, Smallegpad 5, 3800 BP Amersfoort, The Netherlands

<sup>g</sup> Institute of Heritage Sciences (Incipit), Consejo Superior de Investigaciones Cient ficas (CSIC), Santiago de Compostela, Spain

<sup>h</sup> Research Group for Terrestrial Palaeoclimates, Max Planck Institute for Chemistry, Hahn-Meitner-Weg 1, 55128 Mainz, Germany

## ARTICLE INFO

## Keywords:

Fire use  
Diagenesis  
Fireplaces  
Upper Palaeolithic  
Fuel

## ABSTRACT

While the use of fire has long been recognised as a crucial innovation in the cultural evolution of humankind, much research has focused on the (debated) chronology of its earliest use and control, and less on the ways in which fire was used in the deep past. At its latest by the Upper Palaeolithic, hunter-gatherers routinely used fire to heat a wide range of materials, adjusting parameters like temperature, exposure time and fuel type to the specific requirements of the treated materials, for instance in food preparation or tool production.

Comparing analyses of the chemical and physical properties of modern materials, heated under a range of controlled conditions in a laboratory, to archaeological ones might allow the reconstruction of the “heating history” of excavated materials and hence to infer the function of particular fires in the past - provided changes affecting the properties of the heated archaeological material during burial time are taken into consideration. To investigate the feasibility of such an approach, heated materials sampled from ~40,000 to 25,000 year old fireplaces (hearths) and their sedimentary matrices from the Upper Palaeolithic Abri Pataud rock shelter in South-Western France are used here to study (1) the fuel type(s) used by the site's occupants, (2) the temperatures reached in fireplaces and (3) the potential changes in human activities related to fireplaces over time, with the influence of post-depositional processes taken into explicit consideration throughout. For this purpose, we used a range of methods to analyse macroscopically visible as well as “invisible” (microscopic and molecular) heat-altered materials.

The results suggest that charred organic materials (COM) encountered in the samples predominantly result from the fuel used in fireplaces, including the earliest reported use of dung as fuel. Earlier suggestions about the use of bone as fuel at the Abri Pataud are not supported by this study. The heating temperature of COM increased gradually from 350 °C in the Aurignacian to 450 °C in Gravettian levels. Py-GC-MS studies identified a range of organic compounds, biomolecules derived from plant as well as animal sources, still preserved in the sediments after exposure to heat and burial in the rock shelter more than 20,000 years ago. Mammalian mtDNA was identified in sediment samples retrieved from the fireplaces, including ancient mtDNA fragments that originated from one or more modern human-like mitochondrial genome(s). This makes the Abri Pataud the first archaeological site for which ancient modern human mtDNA has been retrieved from sediment samples.

The absence of specific organic compounds (furans) in the Aurignacian levels and their presence in the Gravettian ones, the changes in temperatures reached through the Aurignacian-Gravettian sequence as well as changes in the character of the fireplaces (presence/absence of lining river pebbles) suggest that the functions of hearths changed through time.

\* Corresponding author.

E-mail address: [w.roebroeks@arch.leidenuniv.nl](mailto:w.roebroeks@arch.leidenuniv.nl) (W. Roebroeks).

<sup>1</sup> Deceased, December 29<sup>th</sup>, 2018.

<https://doi.org/10.1016/j.jasrep.2020.102468>

Received 15 April 2020; Received in revised form 22 June 2020; Accepted 2 July 2020

Available online 31 July 2020

2352-409X/  2020 The Author(s). Published by Elsevier Ltd. This is an open access article under the CC BY license

(<http://creativecommons.org/licenses/by/4.0/>).

These results highlight the potential of multi-proxy analyses of macro- and microscopic traces of ancient fireplaces, and especially of a shift in focus towards molecular traces of such activities. Systematic sampling of fireplaces and their sedimentary matrix should become a standard part of the excavation protocol of such features, to improve our understanding of the activities of humans in the deep past.

## 1. Introduction

### 1.1. Fire and human evolution

There is general agreement that heat, generated by fire, formed an important part of the technological repertoire of early humans, with the control of fire playing a crucial role in the development of the human niche. Extant hunter-gatherers use fire to improve their living conditions on the site level - e.g. for thermoregulation, food preparation and providing light (e.g. [Wrangham, 2009](#)) - as well as in the landscapes they inhabit, to increase the quality of resource patches there ([Scherjon et al., 2015](#)). Fire is also thought to have impacted the intensity and possible content of human social interactions, including the development of human language ([Wiessner, 2014](#)). The wide-ranging benefits of fire use are very well-known, and extensively discussed by e.g. [Carmody et al. \(2010, 2011\)](#), [Carmody and Wrangham \(2009\)](#) and [Wrangham \(2009, 2013\)](#), while the various costs of fire use received less attention thus far (but see: [Aarts et al., 2016](#); [Henry et al., 2018](#)).

Recent years have seen a heated debate about the antiquity of the use and control (including production) of fire, with hypotheses varying from a very early (*Homo erectus*) dependence on this tool (e.g. [Wrangham 2009, 2013](#)), to a range of later appearance dates, mostly centered on the middle part of the Middle Pleistocene ([Roebroeks and Villa, 2011](#); [Shimelmitz et al., 2014](#)), but including much younger (Late Pleistocene) estimates ([Dibble et al., 2018](#)). In fact, research of prehistoric fire use may indeed have been "...overly preoccupied with the earliest occurrences of fire rather than its use in cultures where we have long known controlled fire use to be present" ([White et al., 2017](#): p. S288).

With a significant number of studies focused on the chronology of fire use (see [Hlubik et al., 2019](#), for a recent contribution), the reconstruction of the former heating conditions at archaeological fireplaces and of the specific use of the tool have received less dedicated attention thus far, certainly when compared to technological studies of lithics, metals or ceramics in other domains of archaeology. Most studies are mainly concerned with fuel use and with the character of the materials that were exposed to heat in former fires and focus on the analysis of macroscopically visible traces of fire use at archaeological locations ([Aldeias et al., 2012, 2016](#); [Costamagno et al., 2005](#); [Costamagno et al., 2010](#); [Théry-Parisot, 2002](#); [Théry-Parisot and Costamagno, 2005](#); [Théry-Parisot et al., 2009](#); [Théry-Parisot and Henry, 2012](#); [Villa et al., 2002](#)), while relatively few studies have been done on the analysis of microscopic remains, such as charcoal particles ([Marquer, 2010](#); [Marquer et al., 2010, 2012, 2015](#); [Marquer and Otto, in press](#); [Théry-Parisot et al., 2018](#)) and phytoliths ([Wroth et al., 2019](#)) or of biomolecules ([Brittingham et al., 2019](#); [Collins et al., 2017](#); [Kedrowski et al., 2009](#); [Lejay et al., 2016, 2019](#)) (see also [Berna et al., 2012](#)).

In the present study, we aimed to obtain insights in the functions of prehistoric fireplaces and hence the behaviour of the people who created them. Residues from a fireplace correspond to all sizes of physical heat altered materials (from macroscopic fragments to bio-signatures, e.g. molecular markers and indicators). Hence, a reliable assessment of the types of human activities related to the use of heat should consider all types of "artefacts" that can be found within a fireplace. For this purpose, we apply a range of chemical and physical analytical techniques to determine the properties of these macroscopically visible as well as "invisible" (microscopic and molecular) artefacts recovered during archaeological excavations of prehistoric fireplaces. Our

analyses focus on a well-documented series of Upper Palaeolithic fireplaces (hearths) from the Abri Pataud rock shelter site in Les Eyzies-de-Tayac, in the Périgord area of South-Western France.

### 1.2. Fire, a chemical process

Fire is a chemical process, the result of an interaction between heat from an external heat source, fuel and air – the three basic elements of the fire triangle ([Emmons and Atreya, 1982](#)). Fuel is composed of water, inorganic material (ash fraction) and organic material. The organic fraction contains the energy that can be converted into heat. To allow ignition, an external heat source must be introduced to the fuel, for which friction and sparks can be used ([Sorensen et al., 2014](#)). The generated heat will be absorbed by the fuel which is thereby heated causing a gradual change in chemical composition of the organic constituents of the fuel by the formation of a progressively carbon-rich matrix ([Braadbaart et al., 2004](#); [Braadbaart et al., 2007](#); [Braadbaart and Poole, 2008](#)). When a temperature of 280 to 300 °C is reached, the organic fraction will have been transformed into a new, carbon richer, product, mainly consisting of aromatic compounds. As a result, two new products are produced: a solid residue, the char, and simultaneously several volatile gases. This endothermic process will occur completely independent of the supply of air and is referred to as charring ([Braadbaart et al., 2007](#); [Rein 2009](#)). However, as soon as air is present in suitable quantities, both new products will oxidise. The oxidation of the char and the volatiles (producing the characteristic flames) is a highly exothermic process, meaning that a considerable amount of heat will be generated and released ([Rein, 2009](#); [Shafizadeh, 1975](#)). These are the chemical steps towards the combustion or burning processes. After complete oxidation the residue of the fuel is composed exclusively of ash. Since the bio-apatite fraction of bone tissue does not contain organic carbon, bone consists of a relatively large ash fraction compared to plant material ([Reidsma et al., 2016](#)).

### 1.3. Post-depositional processes

Once heated materials enter the archaeological record, they are exposed to a range of post-depositional processes that affect their preservation. At a macroscopic scale these include processes such as trampling and frost action, resulting in fragmentation and movement of materials ([Chravzev et al., 2014](#); [Lyman, 1994](#); [Miller et al., 2009](#); [Théry-Parisot et al., 2010](#)). At a microscopic scale heated materials are affected by chemical weathering (i.e. diagenesis), either resulting from microbial action or from the chemicals present in the depositional environment. Diagenesis can have three main effects on heated materials: it can cause contamination by exogenous minerals, degradation and loss of material, and structural and molecular alteration ([Behrensmeier et al., 2000](#)). Since the effect is dependent on the physical and chemical properties of the original material, different fire proxies and materials heated to different temperatures may be affected in distinct ways ([Braadbaart et al., 2009](#); [Adamiano et al., 2013](#)). Diagenesis may therefore result in a preservation and interpretation bias and influence the reliability of reconstructions of fire-related hominin behaviour. In order to deal with this, this study takes into account the effect of pH on the studied materials, as a measure of the chemical composition of the depositional environment. Different depositional environments (acidic, neutral, alkaline) will have a distinct effect on specific materials. Acidic environments will preferentially transform and dissolve materials such as bone mineral, ash, and lipids ([Karkanas et al., 2000](#); [Pestle 2010](#);

Weiner 2010). In contrast, organic materials such as char and collagen are preferentially affected in alkaline conditions, resulting in dissolution and fragmentation (Braadbaart et al., 2009; Collins et al., 2002). In addition, alkaline environments may deteriorate siliceous materials such as phytoliths (Canti and Huisman, 2015; Xiao et al., 2001). For the current study, the effect of alkaline conditions is of particular importance as Abri Pataud is situated in a limestone-rich environment. Furthermore, it has been shown that wood ash is highly alkaline (pH 9–13) (Etiegni and Campbell, 1991), which may preferentially affect heated materials.

1.4. The remit of this study

Measuring the actual chemical and physical properties of excavated heated materials, and determining the characteristics of the fire they were exposed to (e.g. temperatures and oxygen availability), might enable archaeologists to infer the types of activities related to the use of fire, provided that taphonomic changes affecting the properties of the heated materials during burial time are taken into consideration. Comparing the results of modern materials heated under a range of controlled conditions (e.g. Braadbaart and Poole, 2008; Reidsma et al., 2016; van Hoesel et al., 2019) to archaeological ones makes it possible to reconstruct the “heating history” of excavated materials and hence to infer the function of particular fires in the past.

The objective of the current study is to test whether such an approach is feasible. The Abri Pataud sequence provides an excellent opportunity because of the detail of recording at this rich multi-level site, the relatively high number of hearths excavated and sampled, the ~20,000 years of time covered by the Aurignacian and Gravettian occupations of the site, as well as the fact that the levels are generally

well-separated from each other by virtually sterile Eboulis layers.

We focused our multi-proxy study of the contents of the hearths from the Abri Pataud rock shelter on the following aspects: (1) the influence of post-depositional processes, (2) the fuel type(s) used by the site’s occupants, (3) the temperatures reached in fireplaces and (4) the potential changes in human activities related to fireplaces over time.

2. The Abri Pataud site

The Abri Pataud rock shelter is situated in the village of Les Eyzies-de-Tayac at the foot of a large west-southwest facing limestone cliff flanking the river Vézère. A 1953 test excavation by H.L. Movius revealed a very rich stratigraphic sequence of Upper Palaeolithic deposits, the focus of large-scale excavations between 1958 and 1964. The results of these excavations (Movius, 1965a,b, 1966, 1975, 1977) testify to the multidisciplinary approach of the Abri Pataud project. Movius’ meticulous and well-documented (Nespoulet and Chiotti, 2007) excavations unearthed a rich sequence of in total 9.25 m of Upper Palaeolithic deposits upon the bedrock (Fig. 1), subdivided in fourteen discrete archaeological levels (or couches), contained within sterile Eboulis deposits, limestone debris resulting from solution and frost weathering of the ceiling and walls of the rock shelter. From top to bottom these comprise Level L1 (Solutrean), Levels L2 – L5 (Gravettian), Levels L6 – L8 (Evolved Aurignacian) and L9 – L14 (Early Aurignacian). The formation of the sterile Eboulis layers may have impeded possible post-depositional mixing between the various Levels, although it needs to be mentioned that in some Eboulis layers fire proxies were identified too, in the form of ash layers (Movius, 1966).

The Abri Pataud sequence has been the object of a variety of dating studies, most recently by Higham et al. (2011) and Douka et al. (2020),

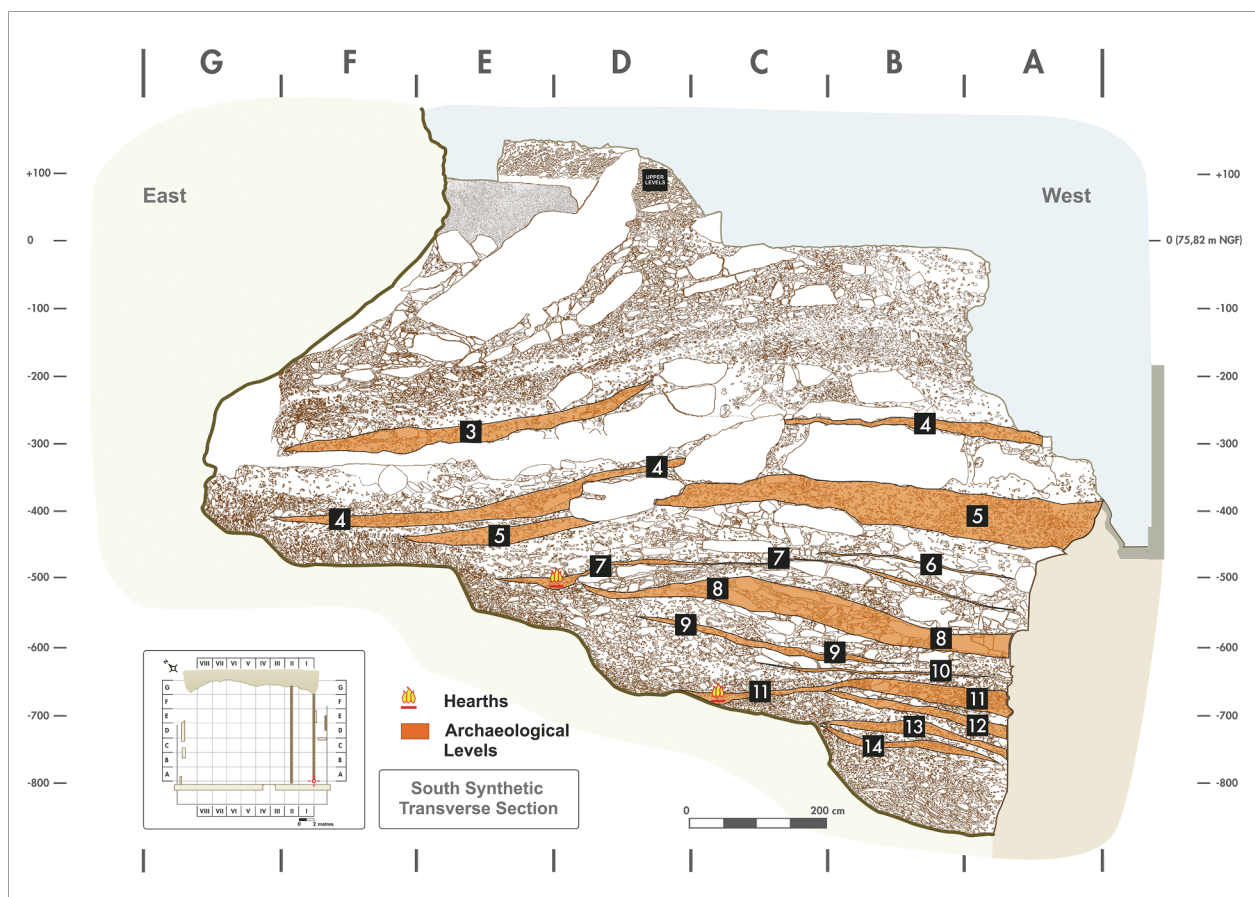


Fig. 1. Cross section of the excavated levels at the Abri Pataud site (drawing R. Nespoulet and L. Chiotti, graphic by Claude Lecante). Numbers in black boxes refer to Level numbers within the Abri Pataud sequence, separated by sterile layers.

with more than 100 radiocarbon dates obtained, situating the deposition of the 9.25 m of deposits between 40,000 Cal BP and the Last Glacial Maximum, of around 20,000 years ago. All archaeological levels are characterised by high concentrations of dispersed ash sediments (Marquer et al., 2010). In most archaeological levels several fireplaces, referred to as hearths by Movius, were found and excavated, varying in shape, size, structure and fill constituents, with in total 52 hearth structures documented (Table 1) (Movius, 1965a,b, 1966, 1975, 1977). Level 1 (Solutrean), Level 2 (Final Gravettian) and Level 13 (Early Aurignacian) did not yield hearths. The excavation of the hearth features followed a basic plan of dividing them along their longest horizontal axis, excavating one half and recording the created section, i.e. the depth and shape of the feature, as well as any manuports encountered (Movius 1977). Photographs of the excavation of these hearth features were included in the publication of the excavation data, with additional photographs included in a typology of the hearths (Movius, 1965a,b, 1966). The fill of the features was systematically sampled and kept in glass jars, today still stored at the Musée de l'Abri Pataud in Les Eyzies. The contents of these jars include heated materials like charred organic material (COM), bone tissue, ash and sediments.

The main hearths documented at Abri Pataud were circular or oval, basin shaped, with a surface area of between 450 and 18,000 cm<sup>2</sup> and a depth of 5–20 cm (Chiotti, 2005; Marquer et al., 2010). In the Gravettian and Aurignacian levels hearths were mainly basin shaped, whereas in Gravettian levels L4 and L5 “bonfire” types were observed. The basin shaped types are rather shallow (3–8 cm) with a diameter in the order of 80 cm. Fig. 2 gives an example of the spatial distribution of a complex of hearths in the Early Aurignacian Level 11, also showing the presence of two dug pits.

During the time period covered by the Abri Pataud sequence, the rock shelter evolved and its back wall and cliff face retreated, as testified by the Eboulis deposits and – dramatically – by the episodes of rock fall visible in the sequence (see Fig. 1). Establishing the distance of fireplaces to the contemporaneous back wall of the shelter is hence not possible. In line with the retreat of the rock wall, the distribution maps published by Movius show a gradual eastward shift (toward the cliff

face) of the location of fireplaces during the Aurignacian and the Gravettian. All of the fireplaces discussed here were situated within the rock shelter, none outside of the *abri*.

The hearths contained a variety of heated remains, including ash, heated bone fragments and some charcoal (Marquer et al., 2010). Movius' team systematically bulk sampled the contents of these hearths, which was referred to as the “fill” (Movius, 1977), the term we use in this study too.

The abundance of heated bone within the Abri Pataud hearths is striking (Marquer et al., 2010; Théry-Parisot, 2002), and has led to suggestions that bones constituted a major fuel during the Upper Palaeolithic here (see below, Discussion Section 5.3).

Within some hearths and/or in their immediate surrounding heated and non-heated river pebbles were recovered (Movius, 1965a, 1965b, 1966). Many of the stones were red or black in colour and/or broken, presumably as a result of heat. From L3 until L8 (Gravettian and Evolved Aurignacian) a considerable number of these stones was found, while deeper in the sequence, from L9 to L14 they were rare or not present at all.

Other indications of the former presence of fire in the form of dispersed ash lenses, heated bones and other hearth debris were excavated in archaeological Levels L2, L6, L9, L10 and in Eboulis 6/7 (E6/7). The application of heat by the occupants was also observed through the presence of ashy material, heated stones, etc. in E5/6 and E13/14. In summary, out of the 26 archaeological and Eboulis levels the effects of heat were observed in 17 Levels (~65%), while only one archaeological level (L13) did not contain any traces of the effect of heat.

### 3. Materials and methods

#### 3.1. Materials

Steered by quantity and availability of well-documented material, either directly obtained from the current sections (by L.M.) or stored in the glass jars, we could use samples from 18 hearths (Table 2) originating from six of the eleven archaeological levels (L4, L5, L7, L8, L11,

**Table 1**

Summary of hearth-related information from Movius (1965a, 1965b, 1966, 1977). L = Archaeological level, E = Eboulis. Dates are from Higham et al. (2011) and Douka et al. (2020). Culture attributions are from Chiotti (2005) and Nespoulet (2008). Presence/absence of other indications of fire, like ash spread, heated bones and hearth debris, are given as well. Presence of river stones around or in hearths is also indicated.

Layers	Culture	Date <sup>14</sup> C BP 2 σ	Hearths (n =)	Other fire proxies	River stones
L2	Final Gravettian	25900–26880	0	yes	yes
E 2/3	–	–	0	yes	no
L3	Recent Gravettian	27770–28580	6	yes	yes
E 3/4	–	–	1	no	yes
L4	Middle Gravettian	29210–31260	11	yes	yes
E 4/5	–	–	0	no	yes
L5	Early Gravettian	30910–33290	6	yes	yes
E 5/6	–	–	0	yes	yes
L6	Evolved Aurignacian	34960–37460	1 remnant	yes	no
E 6/7	–	–	1 remnant	yes	no
L7	Evolved Aurignacian	35400–38730	6	yes	yes
E 7/8	–	–	0	no	no
L8	Evolved Aurignacian	35010–38850	2	yes	yes
E 8/9	–	–	0	no	no
L9	Early Aurignacian	36750–39370	1 remnant	yes	yes
E 9/10	–	–	0	no	no
L10	Early Aurignacian	36970–39950	1 remnant	no	no
E 10/11	–	–	0	no	no
L11	Early Aurignacian	37590–40690	7	yes	few
E 11/12	–	–	0	no	no
L12	Early Aurignacian	37750–40960	4	yes	few
E 12/13	–	–	0	no	no
L13	Early Aurignacian	37670–41840	0	no	few
E 13/14	–	–	0	yes	few
L14	Early Aurignacian	38100–42080	5	yes	few
Basal E	–	–	0	no	few

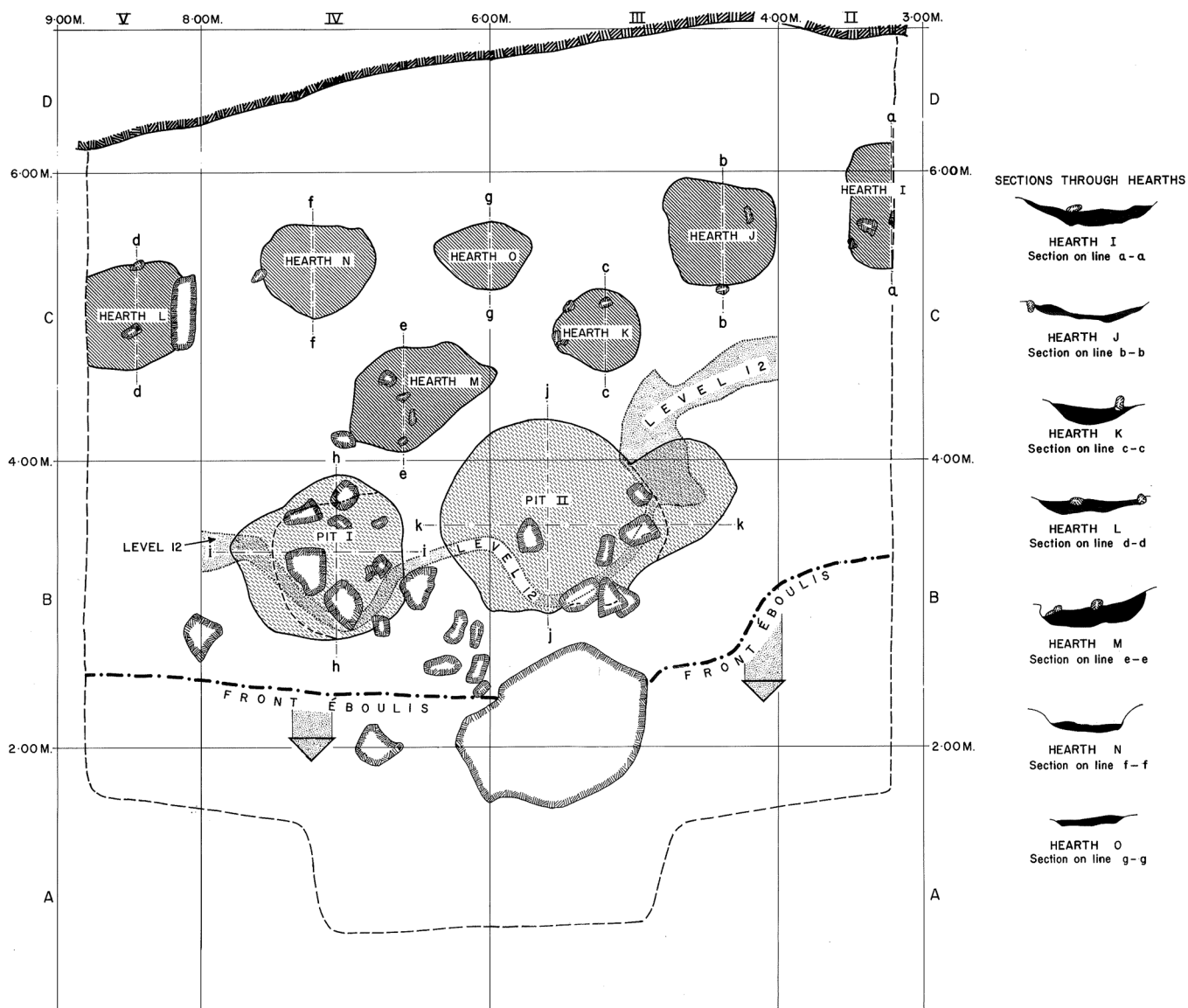


Fig. 2. Archaeological Level 11 (Early Aurignacian), with the location and the dimensions of hearths and two pits situated within the site’s excavation grid system (source: Movius, 1977: Figure 33).

L12 and L14). In the first place this concerns samples of COM and bone tissue larger than around one mm in size, sampled and documented in the field from fireplaces in existing sections and provided for this study by Marquer et al. (2010). The second category consists of materials from the fill that were identified microscopically, such as phytoliths, char and heated bone. We obtained this material from the hearths’ fill collected by Movius and his team, subsequently stored in closed glass containers in the Abri Pataud Museum in Les Eyzies. From the twenty-three available jars, eight jars from different archaeological levels were sampled. From this material the few pieces of COM and bone tissue larger than one mm were removed by hand, and not analysed further. After mechanically sieving the material to a fraction smaller than 200 µm, this fine fraction was used for microscopic work, the study of chemical and physical properties, as well as for analysis of sedimentary mtDNA.

For pH measurements, sediment samples were taken from levels 2, 4 and 11, i.e. from the upper, middle and lower part of the sequence and from the local limestone, in September 2013. In addition, sediment samples were taken from Movius’ jars containing hearth fill material from five archaeological levels (L4, 7, 11, 12, 14).

### 3.2. Methods

#### 3.2.1. Introduction

Following the results of previous work (Reidsma et al., 2016; van Hoesel et al., 2019) we used a combination of techniques to obtain information on the conditions under which the archaeological materials were heated: i.e. structural morphology, colour, reflectance, Thermogravimetric analyses (TGA), Fourier-Transform Infrared Spectroscopy (FTIR), Pyrolysis Gas Chromatography-Mass Spectrometry (Py-GC-MS), X-Ray fluorescence (XRF) and X-Ray diffraction (XRD). Ashes and sediment matrices from fireplaces were studied by recording phytoliths, calcium oxalate crystals, flint chips and fecal spherulites microscopically, measuring sediment pH, using Py-GC-MS to identify biomarkers and screening sediment samples for traces of mtDNA.

In order to establish the heating conditions of the archaeological materials, several reference datasets were used that describe the pathways in which physical and chemical changes occur in organic materials in response to heat and oxygen availability, and hence the changes in the properties of the materials before they became part of the archaeological record. The reference datasets were built using modern samples heated to a range of temperatures and in varying oxygen levels,

**Table 2**

Details of the samples/hearths used in this study. Cultural attribution (see Table 1) MG: Middle Gravettian; EG: Early Gravettian; EVA: Evolved Aurignacian; EA: Early Aurignacian. Hearth labels, locations and characteristics are from Movius (1977), except hearth a in Level 4, directly sampled from existing section by Marquer et al. (2010). COM: charred organic material; Bone: heated bone tissue; Fill (jar nr): material < 200 µm preserved in jars with specific identification numbers, jars are archived at the Abri Pataud Museum; Not known or not available: “-”; Present: “X”; LM: Laurent Marquer; Mov: Movius.

Level	Cult	Hearth	Locat.Tr/Sq	Illustr in Mov 1977	Sampled by:	Area (cm)	Depth (cm)	Shape	COM	Bone	Fill (jar nr)
L4	MG	a	V/F-G	–	LM	–	–	–	X	X	–
	MG	A	III/E-F	Fig 16, Pl 41	Mov	80–50	–	basin	X	X	7,8,6
	MG	B	III/E	Fig 16	Mov	30–10	–	basin	–	X	9
	MG	D	III/E	Fig 16, Pl 42	Mov	110–90	–	basin	–	X	12,13
	MG	E	III/E	Fig 16	Mov	50–40	–	basin	X	X	14
L5	EG	K2	IV/E	Fig 29, Pl 55	Mov	100–140	7	basin	X	X	6
	EG	J1	IV/E	Fig 28, Pl 52	Mov	120–350	2–6	bonfire	–	X	9,11a,11b
L7	EVA	Y	IV/D-E	Fig 30, Pl 61	Mov	70–90	10	basin	X	X	–
	EVA	W1	IV/D-E	Fig 30, Pl 60,61	Mov	80–90	5	basin	–	X	12
	EVA	W2b	IV/D-E	Fig 30, Pl 62	Mov	130–150	20	basin	X	X	4,5,16
L8	EVA	A	III/C	Fig 32, Pl 63,64	Mov	50–50	17	basin	X	X	4
L11	EA	I	II/C-D	Fig 33, Pl 66	LM	30–80	15	basin	X	X	–
	EA	I	II/C-D	Fig 33, Pl 66	LM	30–80	15	basin	–	X	–
	EA	L	V/C	Fig 33, Pl 66	LM	70–70	15	basin	X	X	9
L12	EA	P	II-III B	Fig 34	Mov	68–74	15	basin	–	–	3
L14	EA	T	IV/B	Fig 35, Pl 73,74	Mov	47–47	8	basin	–	X	2a,2d
	EA	V	II-III/B	Fig 35, Pl 76	Mov	56–64	10	basin	X	X	10,13
	EA	Ω	III/B	Fig 35, Pl 77	Mov	60–76	6	basin	X	X	16a

under controlled conditions in a laboratory setup. Included are charred plant material (Braadbaart and Poole 2008; Braadbaart 2004), heated bone (Reidsma et al., 2016; van Hoesel et al., 2019), and ash from different fuels (Braadbaart et al., 2012). In addition, reference data on the effect of pH on heated materials was used (Braadbaart et al., 2009; Reidsma, in prep.).

### 3.2.2. Macroscopically visible heat altered materials

#### 3.2.2.1. Charred organic material (COM)

3.2.2.1.1. *Structural morphology*. From eleven of the seventeen sampled hearths enough charcoal or other charred organic material was available for study (Table 2). For the analyses three randomly selected specimens of each of the eleven samples were embedded in a separate resin block and polished in accordance with standard methods as defined in ISO 7404, part 2 (1985). The structural morphology of these samples (Table 2) was examined under reflected light and oil immersion using a Leitz DMLA microscope equipped with a motorised xyz-stage and a Basler video camera.

3.2.2.1.2. *Reflectance measurements (%Ro)*. In order to determine the temperature each specimen had been subjected to, reflectance measurements were performed on the polished samples embedded in resin (See for details Braadbaart and Poole, 2008). Reflectance was measured under oil immersion at a wavelength of 546 nm using the Leitz microscope. For each sample a total of at least 100 randomly performed reflectance readings were taken and the mean reflectance calculated. Reflectance measurements were performed in accordance with standard methods defined in ISO 7404, part 5 (1994). Past heating temperatures were determined using the calibration curves as developed by Braadbaart and Poole (2008).

3.2.2.1.3. *Fourier transform Infrared Spectroscopy (FTIR)*. Single measurements were performed on powders of COM using an Attenuated Total Reflectance (ATR) Perkin Elmer Spectrum100 FT-IR spectrometer, equipped with a diamond ATR crystal. Absorption spectra were accumulated in 16 scans, for the 4000–450 cm<sup>-1</sup> wavelength range, with a spectral resolution of 4 cm<sup>-1</sup>. All spectra were background corrected and normalised to their highest peak.

3.2.2.1.4. *Pyrolysis mass Spectrometry (Py-MS)*. Single measurements of powdered material were taken using a Frontier Lab 3030D pyrolyser coupled with a ThermoScientific Focus GC and ISQ mass spectrometer. The pyrolyser heated the sample from 70 to 800 °C at a heating rate of 100 °C /min. The EGA GC chamber was kept at a constant temperature of 300 °C. The mass spectrometer scanned from

20 to 4000 AMU using a cycle time of 7 scans per second. Data acquisition and processing were performed using Xcalibur 2.1 software.

#### 3.2.2.2. Heated bone tissue

3.2.2.2.1. *Preparation of samples for XRF, XRD, FTIR and TGA analyses (see following subsections)*. The different types of bone, i.e. cortical and cancellous, were identified macroscopically. At first, from each of the seventeen investigated hearths, the dark and light coloured samples were selected. Individual pieces were powdered in an agate mortar and analysed using XRF, XRD and FTIR, after which material was retrieved as much as possible for further analyses. Finally, the powdered material was used for TGA and Py-GC–MS, which are destructive methods. Pyrolysis-MS was applied following the same protocol as for COM materials (see above). Whenever sample volume was insufficient for TGA, five individual samples were randomly selected (dark vs. light coloured) and mixed prior to analysis.

3.2.2.2.2. *X-Ray fluorescence (XRF)*. The XRF analyses were carried out using a Thermo Scientific Niton XL3t GOLDD + energy-dispersive p-XRF analyzer, equipped with a silicon drift detector. Samples were homogenised in an agate mortar and compressed manually with the agate pestle in a PE-ring with a height of 10 mm. Analyses were performed using a stand mounted above the sample ring. In this way no separation foil between the sample and the XRF was needed, that could absorb secondary X-ray's from light elements. The Cu/Zn-mining mode was used, with a measuring time of 110 s, using 4 sequential energy settings: Light range (Mg to Cl) at 8 kV 200 µA, low range (K to Ti) at 20 kV 100 µA, main range (V to Ag including L-lines for Pb) and high range (Cd- Ba) both at 50 kV, 40 µA. Since factory calibrations are a potentially serious source of error when using HH XRF, the machine calibration was checked and adapted using a set of 14 powdered ISE standard soil samples (www.wepal.nl). Accuracy was tested using the BAMS005B glass standard.

3.2.2.2.3. *X-Ray diffraction (XRD)*. Powdered samples were attached to an amorphous silica plate using resin. Analysis was carried out on two different machines: a Bruker D8 Discover XRD equipped with a 2D General Area Detector Diffraction System (GADDS) detector and a Philips PW1200. Both devices use a copper target X-ray tube (8 mm) and were operated at 40 kV and 30 mA. The measurements on the Bruker were collected in the 16–68° 2θ range, those on the Philips between 20 and 70° 2θ, both with a step size of 0.04° 2θ and a step time of 5 s. Spectra were background corrected and normalised to their highest peak. The XRD-crystallinity index (CI) was determined

using the equation of [Person et al. \(1995\)](#).

**3.2.2.2.4. Fourier transform Infrared Spectroscopy (FTIR).** For the method see above. The FTIR splitting factor (SF) is calculated using the heights of the  $559\text{ cm}^{-1}$  band, the  $599\text{ cm}^{-1}$  band and the trough separating the two bands as explained in e.g. [Weiner and Bar-Yosef \(1990\)](#) and [Munro et al. \(2007\)](#). All heights are measured above a local baseline drawn between  $750$  and  $450\text{ cm}^{-1}$ .

**3.2.2.2.5. Thermo-gravimetric analysis (TGA).** TGA was performed on one gram of powdered sample, using a LECO TGA 701 machine. Samples were heated to  $950\text{ }^{\circ}\text{C}$  with a heating rate of  $5\text{ }^{\circ}\text{C}/\text{min}$ . Air was used as the carrier gas to ensure complete combustion. The water content was determined as the relative mass lost at  $200\text{ }^{\circ}\text{C}$ , the organic content as the mass loss between  $200$  and  $600\text{ }^{\circ}\text{C}$ , and the ash content as

the remaining mass at  $950\text{ }^{\circ}\text{C}$ .

### 3.2.3. Microscopically visible heat altered materials

The sediment matrices of each fireplace were examined under polarised light using a Leica DM750 (PLM and XPL) microscope. For this purpose,  $4\text{ mg}$  of each sample was thoroughly mixed with  $2\text{ ml}$  deionized water. The material was not chemically treated. From each mixture,  $0.05\text{ ml}$  was mounted on a glass slide. In this way, each slide contained an equal amount of material, that is,  $0.1\text{ mg}$ , which allowed for a comparison between the different samples. In addition, these slides were examined using *trans*-illumination under a LeicaDM6000 M microscope. Applying both microscopic methods and using the difference in birefringence of polymorphs of silica ([Ulery and Drees, 2008](#)) as

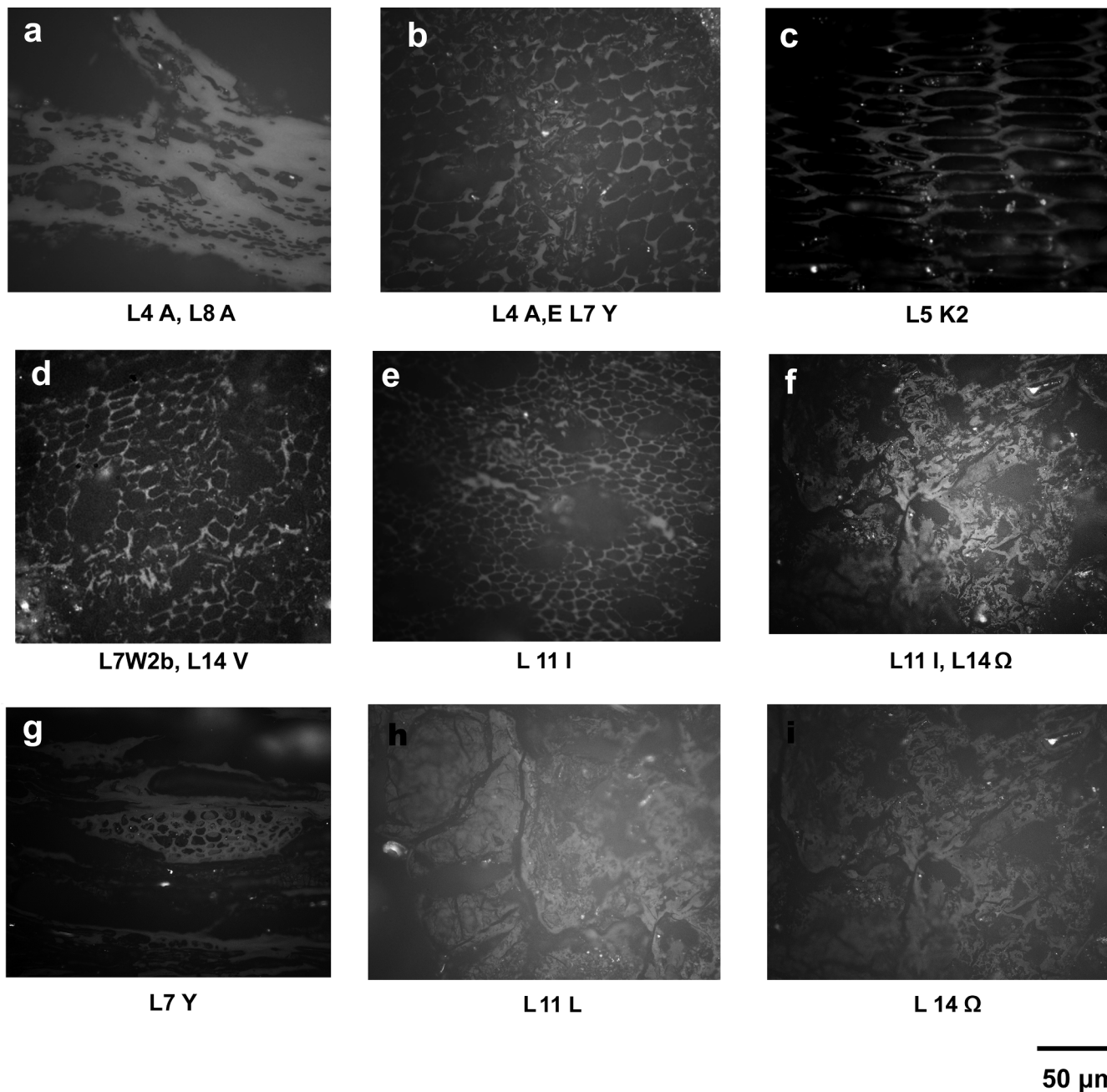


**Fig. 3.** Photographs of structural morphology of charred organic material under reflected light from the eight studied hearths ([Table 2](#)), illustrating the four categories (see core text). (i) Well-preserved wood anatomy (b, g). (ii) Deformed cells and highly fragmented structures (c, d, e). (iii) Homogeneous structures without distinct visible cells (a, f). (iv) Fiber structures that refer to dung or peat (f, h, i). The archaeological levels and labels of each hearth are indicated in each picture.



well as the morphology of the particles, a distinction was made between the various materials that may be present in the fill, including silica phytoliths, calcium oxalate crystals, flint chips and faecal spherulites.

### 3.2.4. Sediment matrix (< 200 $\mu\text{m}$ ).

**3.2.4.1. Sediment pH measurements.** The pH measurements on the sediment and fill samples followed the specifications outlined in NEN 5750, 1989 and were performed using a Consort D514 digital pH meter.

**3.2.4.2. Analytical pyrolysis.** Sediment samples were subjected to mild HCl-HF treatment to concentrate organic matter. Briefly, 1.0 g of material was weighed into 50 ml centrifuge tubes, with the exception of sample L8, for which only 0.2 g was available. Aliquots of 1 M HCl (aq) were added until the reaction was visually interpreted as complete (9–14 ml of HCl, depending on the sample). Next, dilute HF (2%, aq) was added until the 40 ml mark and the suspension was homogenised overnight in an orbital shaking device. After centrifugation (10 min, 2000 rpm), the supernatant was discarded and the HF treatment was repeated. After discarding the second HF supernatant, the residues were washed three times with distilled water (adding H<sub>2</sub>O until 40 ml mark, overnight shaking, and centrifugation cycles). The residue was dried at 35 °C to obtain the final residue for analysis.

Pyrolysis-GC-MS was performed using a Pyroprobe 5000 (CDS Analytical) coupled to an Agilent 6890/5975 GC-MSD. Sample materials were embedded in deactivated fire-polished quartz tubes with deactivated quartz wool on both ends. The pyrolysis set-point temperature was 650 °C, reached at a rate of 10 °C/ms and maintained for 20 s. The pyrolysis interface, the GC inlet and the GC-MSD interface were isothermal at 325 °C. The GC oven was heated from 60 °C (1.5 min isothermal) to 325 °C (3 min dwell time) at a rate of 20 °C/min. Helium was used as the carrier gas at a flow rate of 1 ml/min. The GC was equipped with a HP-5MS (non-polar) capillary column and operated in split mode (1:10). The electron impact (EI) ionisation energy of the MSD was 70 eV and the quadrupole detector scanned in the  $m/z$  range of 50–500.

For Thermally assisted Hydrolysis and Methylation (THM)-GC-MS, an aliquot of aqueous tetramethylammonium hydroxide (TMAH, Sigma-Aldrich, 25%) was added to the sample and allowed to react with the sample for 30 min, before inserting the sample-containing quartz tubes into the pyrolysis instrument, and analysis using the same conditions and parameters as those used for Py-GC-MS, with the exception of longer isothermal initial temperature (5 min) and the use of a solvent delay period of 5 min.

**3.2.4.3. DNA analysis.** Seven sediment samples, collected within ( $n = 6$ ) or adjacent ( $n = 1$ ) to Abri Pataud hearths, were screened for the presence of ancient DNA. The samples originated from levels L4,

L5, L7, L11, L12 and L14. DNA was extracted from between 58 and 92 mg of sediment and purified on an automated liquid handling platform (Bravo NGS workstation, Agilent Technologies) using binding buffer 'D' and silica magnetic bead as described in (Rohland et al., 2018). Aliquots of the DNA extracts were converted into single-stranded libraries (Gansauge et al., 2017). The yield and efficiency of library preparation were determined using quantitative PCR assays and an oligonucleotide spike-in as described in Glocke and Meyer (2017). Libraries were amplified and tagged with double indices (Kircher et al., 2012) and enriched by hybridisation capture for both mammalian mtDNA (Slon et al., 2016) as well as specifically for human mtDNA (Marčić et al., 2010; Fu et al., 2013) prior to sequencing on an Illumina MiSeq. Negative controls for the DNA extraction, purification and library preparation procedures were carried along with the samples. All steps of sample preparation subsequent to DNA extraction were also carried out on the automated liquid handling platform, as described in detail in Slon et al. (2017).

Data processing and analysis followed the scheme described in Slon et al. (2017). In short, after the alignment of reads to a reference genome and the removal of PCR duplicates, sequences spanning at least 35 base pairs were assigned to a taxon of origin at the family level using a 'lowest common ancestor' algorithm (Huson et al., 2007) and evaluated for the presence of nucleotide substitutions typical of ancient DNA (Briggs et al., 2007). DNA fragments identified as originating from Hominidae mitochondrial genomes were retained for further analysis. To distinguish between modern human-, Neandertal-, Denisovan- or Sima de los Huesos-like mtDNA, we recorded the base carried by fragments with evidence of ancient DNA damage at phylogenetically 'diagnostic positions' in the mitochondrial genome (Meyer et al., 2016), i.e. positions where the mtDNA genomes pertaining to one of these groups differed from a chimpanzee mtDNA and the mtDNAs of all other groups.

## 4. Results

### 4.1. Macroscopically visible heat altered materials

#### 4.1.1. Charred organic material (COM)

**4.1.1.1. Structure.** Four distinctive morphological structures are distinguished (Fig. 3). Three of these structures are (i) well-preserved wood anatomy (Fig. 3b and g), (ii) deformed cells and highly fragmented structures (Fig. 3c and e) and (iii) homogeneous structures without distinct visible cells (Fig. 3a and f). Homogeneous structures might be related to the combined effect of the decay of wood due to pathogens before combustion (Henry and Théry-Parisot, 2014), internal pressures due to the evacuation of wood moisture during combustion (Théry-Parisot and Henry, 2012) and/or higher heating

**Table 3**

Results of analyses based on charred organic material (COM). %Ro: Mean reflectance values. Temperatures based on %Ro are according to calibration curves for alkaline conditions (Braadbaart et al., 2009). Temperatures based on FTIR are from Fig. 4. No result = -.

Level	Hearth	Sample label	Sample number	Lab number	Botanical identification	%Ro	%Ro SD	%Ro temp (°C)	Morphology type	FTIR type	PyMS
L4	a	(5–8)3	2	–	Angiosperm	–	–	–	–	–	–
L4	A	01	70	AP 1	<i>Pinus</i>	0.835	0.155	450	I	A	–
L4	A	01	66	AP 2	Angiosperm	1.521	0.168	440	III	A	–
L4	E	03	41–59	–	<i>Pinus</i>	0.716	0.095	440	I	–	–
L5	K2	H301	36–40	AP 3	Angiosperm	0.970	0.117	390	II	C	–
L7	Y	01	3	AP 4	Rhamnaceae	1.010	0.163	390	I	A	–
L7	Y	2–03	77	AP 5	<i>Salix</i>	1.058	0.095	390	I	A	–
L7	W2b	2–03	74–78	–	<i>Salix</i>	0.801	0.124	360	II	–	–
L8	A	0	27–28	–	Rhamnaceae	0.686	0.104	360	III	–	–
L8	A	0	24	AP 6	Rhamnaceae	0.911	0.122	385	III	B	–
L11	I	(1–2)1	60	AP 7	Angiosperm	0.808	0.178	370	II	B	$m/z$ 28; 44
L11	L	(5–8)6	–	–	Not known	0.763	0.128	370	IV	–	–
L14	V	03	61	–	<i>Betula</i>	0.656	0.113	360	II	–	–
L14	$\Omega$	01	1	AP 8	Not known	0.476	0.119	350	IV	A	–

temperatures and the melting of the constituents (Braadbaart et al., 2016). All these samples are considered as charred wood, i.e. charcoal. A fourth (iv) variety of morphological structures corresponds to the absence of wood cells and the observation of fibre structures that relate to dung or peat are present (Fig. 3h and i). This category corresponds to samples from Levels L11 and L14.

4.1.1.2. Reflectance measurements. The mean reflectance values (%Ro) measured on the charcoal samples range from 0.476 in Level L14 to 1.521 in Level L4 (Table 3). To determine the temperatures to which the samples have been heated, calibration curves for various charred wood types were used (Braadbaart and Poole, 2008). The results show that the heating temperatures of the samples range from 350 °C in L14

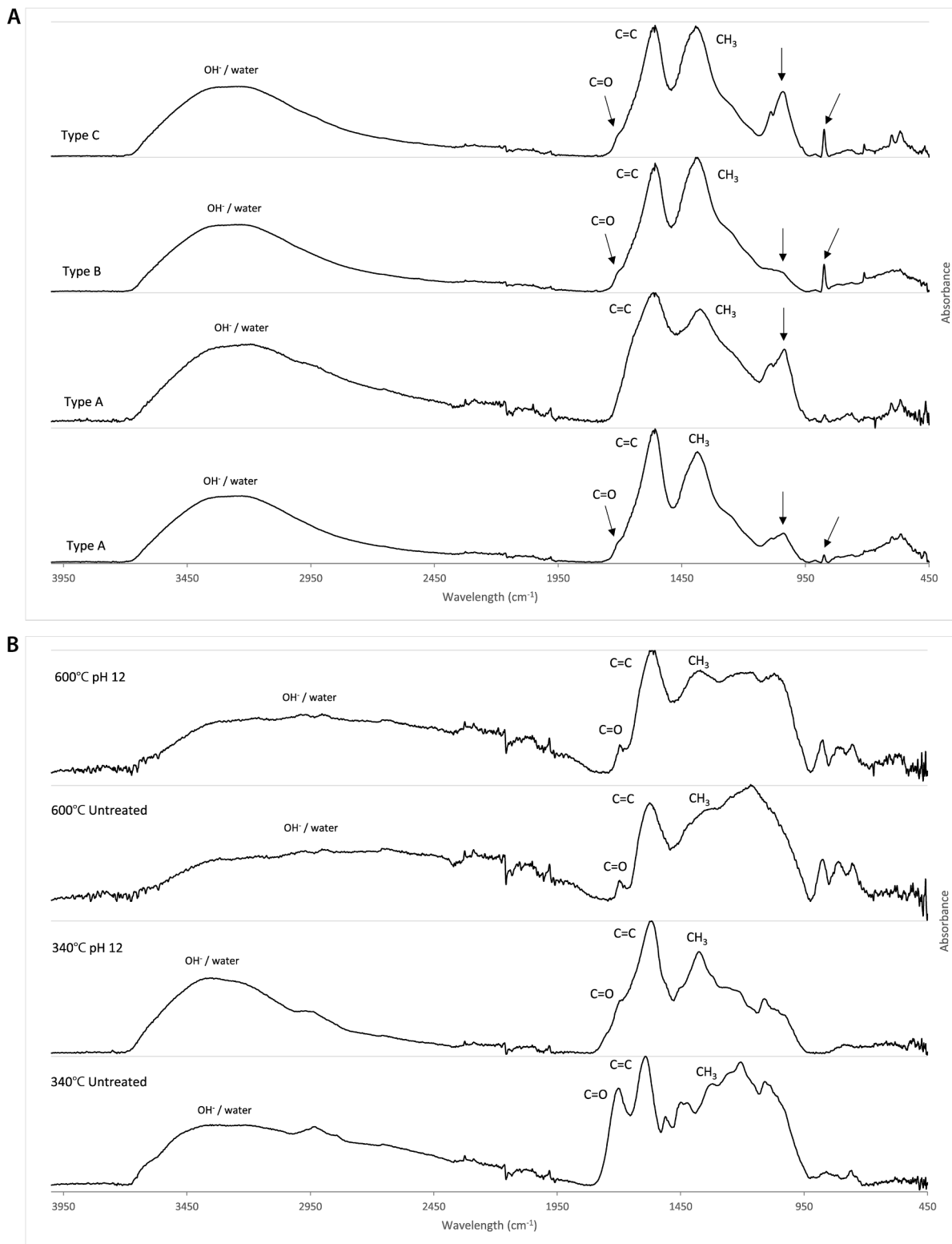


Fig. 4. A: FTIR spectra representative of the three types of COM samples found at Abri Pataud, with the most notable peaks labelled or indicated with an arrow in case of tentative identifications. B: FTIR spectra of modern reference samples both untreated and exposed to alkaline conditions (cf. Braadbaart et al., 2009).

to 450 °C in L4 (Table 3). Fireplaces from L4 record the highest temperatures based on %Ro, in particular for the *Pinus* samples. Note that it is known that charcoal, deposited in an alkaline environment, will give lower reflectance values; corrections have been applied here to determine the temperature (Braadbaart et al., 2009).

**4.1.1.3. FTIR.** The spectra of the eight COM samples from the various hearths are characterised by three main bands i.e. a broad band at around 3400  $\text{cm}^{-1}$  and bands at 1558 and 1385  $\text{cm}^{-1}$  (Fig. 4a). The broad band at 3400 is assigned to  $\text{OH}^-$  stretching vibration (Chowdhury et al., 2016; Guo and Bustin, 1998; Liu et al., 2016). The band at 1558  $\text{cm}^{-1}$  is assigned to aromatic C=C ring stretching vibrations (Chowdhury et al., 2016; Cohen-Ofri et al., 2006; Guo and Bustin, 1998; Liu et al., 2016), while the band at 1385  $\text{cm}^{-1}$  is ascribed to aliphatic  $\text{CH}_3$  deformation (Chowdhury et al., 2016; Guo and Bustin, 1998). In addition to the main peaks, a hump can be observed around 1700  $\text{cm}^{-1}$ , which is assigned to C=O (carbonyl) stretching vibration (Chowdhury et al., 2016; Guo and Bustin, 1998; Liu et al., 2016; Nishimiya et al., 1998). In most samples a peak can also be observed around 1030  $\text{cm}^{-1}$ . While such a peak has been ascribed to C–O stretching in plant material heated to low temperatures (< 320 °C; Kaal et al., 2012; Guo and Bustin, 1998; Oudemans et al., 2007), for the Abri Pataud samples it seems more likely that it results from contamination. Either from phosphates or from the inclusion of humic acids, the latter of which is also supported by the presence of a small peak at 3700  $\text{cm}^{-1}$  (Brinkkemper et al., 2018; Vaiglova et al., 2014). Some COM samples are also contaminated with carbonates, based on the presence of small peaks at 875 and 715  $\text{cm}^{-1}$  (Vaiglova et al., 2014).

In addition, the samples can be characterised by the relative height of the bands at 1558 and 1385  $\text{cm}^{-1}$ . The majority of the samples belong to type A (AP 1, 2, 4, 5, 8), which represents all spectra where the band at 1558  $\text{cm}^{-1}$  has a higher intensity than the band at 1385  $\text{cm}^{-1}$ . Within this category there is variation in the intensity of the band at 1030  $\text{cm}^{-1}$ . Type B (AP 6, 7) is defined by a higher intensity for the band at 1385  $\text{cm}^{-1}$  as compared to the band at 1558  $\text{cm}^{-1}$ . Finally, for type C (AP 3) the bands at 1558 and 1385  $\text{cm}^{-1}$  display the same intensity. Comparison to reference data suggests that the presence of a pronounced peak at 1385 is likely the result of prolonged exposure to alkaline conditions (Fig. 4b). The characteristics of Type B and C are likely explained by the contamination with exogenous carbonates, and result from the overlap of the peak at 1385  $\text{cm}^{-1}$  with the main peak observed in limestone (Vaiglova et al., 2014).

**Table 4**

Mass distribution of available bone tissue samples expressed as total weight (wt) in grams. The percentages of dark and light coloured samples, as well as the rest are shown and expressed as wt%.

Level	Hearth	Sample label	Total weight (g)	Dark colour (wt %)	Light colour (wt %)	Rest (< 2mm) (wt %)
L4	a	(5–8)3	2.12	100	0	0
L4	A	01	34.24	56.3	23.6	20.2
L4	B	04	47.05	62.3	28.5	9.1
L4	D	02	75.94	77.1	13.0	9.8
L4	E	03	5.51	59.6	0	40.4
L5	K2	H301	48.71	72.2	6.2	21.6
L5	J1	J301	4.08	64.3	35.7	0
L7	a	(1–2)1	0	0	0	0
L7	Y	01	2.26	100	0	0
L7	W1	02	14.01	77.4	10.4	12.2
L7	W2b	2–03	3.67	63.0	37.0	0
L8	A	0	2.40	0	100	0
L11	I	(1–2)1	99.57	73.05	17.1	9.9
L11	I	(1–2)5	120.63	69.0	20.9	10.1
L11	L	(5–8)6	83.37	69.3	18.6	12.1
L14	T	01	67.56	74.9	17.0	8.0
L14	V	03	74.78	60.5	23.1	16.4
L14	Ω	01	75.24	75.5	7.9	16.6

**4.1.1.4. Pyrolysis-MS.** A COM sample from Level L11 was measured with PyMS. The chromatogram is characterised by a very low amount of pyrolysis products. Only ions  $m/z$  28 (CO) and 44 ( $\text{CO}_2$ ) are observed. The virtual absence of volatiles and pyrolysis products suggests that this COM had formed under high temperatures, but their rarity may also result from the effects of a high pH (cf. Braadbaart et al., 2009).

#### 4.1.2. Bone tissue samples

**4.1.2.1. Type and colour.** As an illustration of the colour, size and type of bone tissue material, specimens of sample (1–2)1 from Level L11, hearth I, are presented in Fig. 5. Dark and light coloured specimens are observed. In addition, samples are present with a light colour on the outside, while the inside is still dark (arrows in Fig. 5). The overall results show that around 70 wt% of the investigated bone tissue samples is dark coloured, against less than 30 wt% light-coloured material (Table 4).

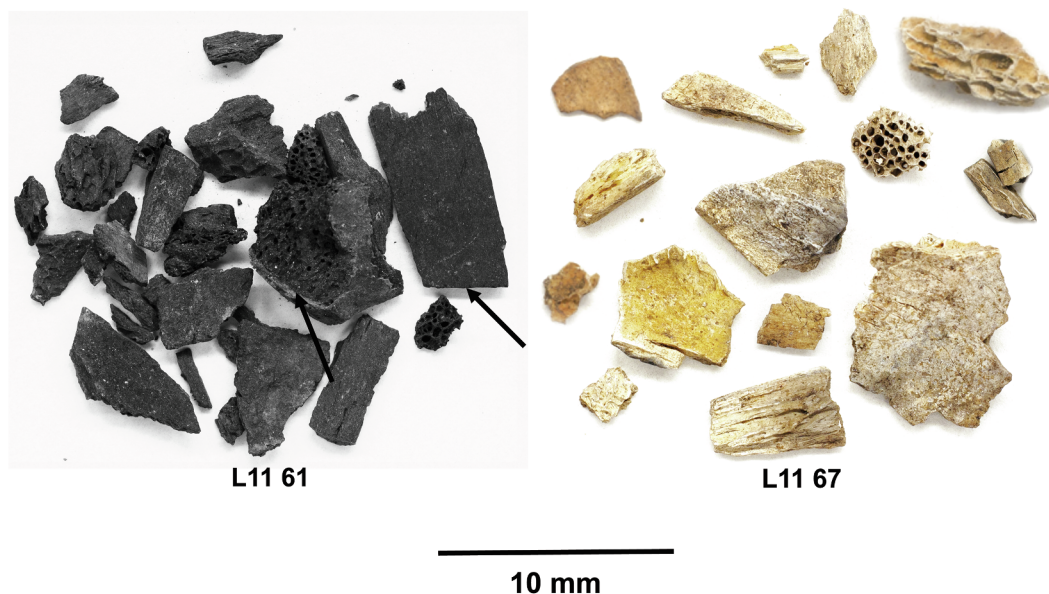


Fig. 5. Samples of dark (L11-61) and light coloured (L11-67) bone tissue samples, from Level 11 (Early Aurignacian), hearth L.

**4.1.2.2. TGA.** The TGA results (Table 5) reveal that the organic fraction of the samples varies for dark-coloured cancellous tissue from 4.7 to 7.1 wt%, and from 5 to 8.1 wt% for the dark-coloured cortical tissue. The organic fraction is lower for light-coloured samples than for the dark ones, with a range of 1.1 to 2.4 wt% for the light-coloured cancellous samples and a range of 0.8 to 2.4 wt% for the light-coloured cortical samples.

**4.1.2.3. XRF.** The XRF analyses (Table 5) show that, while both ranges overlap, the dark-coloured samples on average have a lower Ca and P content than the light-coloured samples (dark: Ca 30–36 wt%, P 13–16 wt%; light: Ca 34–40 wt%, P 15–20 wt%). It should be noted that two samples deviate from this trend: first, the dark-coloured sample from hearth L11-I (AP 11.1) shows results that are more similar to light-coloured samples, i.e. high Ca and P content. In contrast, the light-coloured sample from the large stratified hearth in lens J1 in Level 5 (AP 34.1) is more similar to a dark-coloured sample, i.e. low Ca and P content.

**4.1.2.4. FTIR.** The FTIR results of the bone samples show that all samples (light and dark) can indeed be identified as bone, with bands characteristic of bone mineral (Reidsma et al., 2016). The vibrational modes that originate from the  $\text{PO}_4^{3-}$  ions can be found at  $1020\text{ cm}^{-1}$  (v3 asymmetric stretch), at  $960\text{ cm}^{-1}$  (v1 symmetric stretch), and at  $600$  and  $560\text{ cm}^{-1}$  (both v4 bending). In addition,  $\text{CO}_3^{2-}$  modes can be found at  $1450$  and  $1415\text{ cm}^{-1}$  (v3 asymmetric stretch), and at  $870\text{ cm}^{-1}$ . The latter is tentatively ascribed to  $\text{CO}_3^{2-}$  (v2 out of phase bending) as it could also originate from  $\text{HPO}_4^{2-}$  (v2 bending). It should be noted that most samples appear to have been enriched with exogenous limestone from the depositional environment. This limestone is characterised by a broad dominant peak at  $1397\text{ cm}^{-1}$ , and two narrow peaks at  $870\text{ cm}^{-1}$  and  $713\text{ cm}^{-1}$  (Fig. 6). As a result of this contamination, the morphology and intensity of the  $\text{CO}_3^{2-}$  peaks cannot be reliably used in the reconstruction of the past heating conditions, as they overlap with characteristic limestone peaks. In these cases, focus was shifted to the  $\text{PO}_4^{3-}$  peaks and where present the organic aromatic compounds.

From the FTIR spectra of the dark-coloured samples (Fig. 7) two types can be distinguished that display similar morphology and intensity of the bands. Type A is characterised by a shoulder on the main

phosphate peak, at  $1077\text{ cm}^{-1}$ , and a hump at  $618\text{ cm}^{-1}$ , both likely indicating high temperatures and/or limited availability of oxygen. Comparison with the reference data suggests past heating temperatures of  $700\text{ }^\circ\text{C}$  and higher for type A samples. Type B is characterised by the absence of the features defining type A. Comparison with the reference data suggests past heating temperatures lower than  $700\text{ }^\circ\text{C}$ . For both types weak bands are observed in the range of  $1640$  to  $1550\text{ cm}^{-1}$ , which are assigned to aromatic ring C=C stretching characteristic for charred collagen. Additionally, a broad band can be observed at  $3500$ – $3100\text{ cm}^{-1}$ , which relates to the H–O–H bonds of absorbed water.

From the FTIR spectra of the light-coloured samples (Fig. 7) two types can also be distinguished that display similar morphology and intensity of the bands. Type C is characterised by very reduced  $\text{CO}_3^{2-}$  peaks at  $1450$  and  $1415\text{ cm}^{-1}$  (the former now higher than the latter), a very reduced  $\text{CO}_3^{2-}/\text{HPO}_4^{2-}$  peak at  $870\text{ cm}^{-1}$ , very advanced splitting of the  $\text{PO}_4^{3-}$  peaks, and the presence of hydroxyl ( $\text{OH}^-$ ) peaks at  $3575$  and  $630\text{ cm}^{-1}$ . Type D, on the other hand, is characterised by a similar morphology but higher intensity of the  $\text{CO}_3^{2-}$  peaks at  $1450$  and  $1415\text{ cm}^{-1}$ , a less reduced  $\text{CO}_3^{2-}/\text{HPO}_4^{2-}$  peak at  $870\text{ cm}^{-1}$ , less advanced splitting of the  $\text{PO}_4^{3-}$  peaks, and the presence of hydroxyl ( $\text{OH}^-$ ) peaks at  $3575$  and  $630\text{ cm}^{-1}$ . Comparison with the reference data suggests high past heating temperatures ( $> 600\text{ }^\circ\text{C}$ ) for both types, with type C samples potentially having been heated to higher temperatures than type D samples. In both sample types organic components or bands related to absorbed water were not observed.

**4.1.2.5. Crystallinity using XRD and FTIR.** Crystallinity of each sample has been studied using SF (FTIR) and CI (XRD) (Table 5). For the dark-coloured samples the SF (FTIR) ranges from 3.61 to 4.47, while for the light-coloured samples the range of values is higher, 4.59 to 6.33. The results of the CI (XRD) also show higher values for the light- (0.70 to 1.15) than for dark-coloured samples (0 to 0.43). Nevertheless, comparison with the reference data indicates similar heating temperatures for both colour categories.

**4.1.2.6. Pyrolysis-MS.** The chromatograms of bone samples from archaeological levels L7 and L11 are characterised by low abundance of pyrolysis products, mainly ions  $m/z$  28 (CO) and 44 ( $\text{CO}_2$ ). In addition, samples AP28 (L11, hearth I) and AP35 (L7, hearth W) show

**Table 5**

Results of analyses performed on bone tissue samples and the resulting temperature estimates. Temperature reconstructions (in  $^\circ\text{C}$ ) were made using modern reference data (Reidsma et al., 2016; van Hoesel et al., 2019) and based on best fit with the majority of the analytical techniques, taking the observed effects of high pH into account. \* = missing values due to measurement error.

Level	Hearth	Sample	Lab nr	Colour	Bone type	TGA org wt%	FTIR type	FTIR SF	XRD CI	XRF Ca wt%	XRF P wt%	PyMS ( $m/z$ )	Heating temp. ( $^\circ\text{C}$ )
11	I	F11 (1–2)1	11.1	dark	canc.	7.06	A	4.20	0.12	36.49	15.41	–	700–800
11	I	F11 (1–2)1	11.2	dark	cort.	–	B	3.76	0.03	33.22	*	–	600–700
11	I	F11 (1–2)1	28.3	dark	cort.	–	B	3.72	0.31	33.72	15.61	–	600–700
11	I	F11 (1–2)1	28.4	dark	canc.	–	A	3.85	0.43	29.68	12.98	–	700–800
11	I	F11 (1–2)1	29.1	dark	cort.	6.72	A	4.06	0.09	33.44	15.42	28; 44	700–800
11	I	F11 (1–2)1	30.1 black	dark	canc.	4.69	B	4.00	–	31.06	12.97	–	~700
4	D	F4.D02	31.1	dark	canc.	6.05	A	4.47	6.05	31.18	15.53	–	700–800
5	J	F5.H301	33.1	dark	cort.	5.00	A	4.37	5.00	33.64	12.92	–	700–800
7	W	F7 (1–2)1	35.1	dark	canc.	6.36	B	3.63	6.36	30.11	12.70	28; 44; 78; 91	600–700
14	V	F14V.03	37.1	dark	canc.	4.82	B	3.61	4.82	31.88	14.17	–	500–600
14	V	F14V.03	38.2	dark	cort.	5.60	A	4.02	5.60	34.09	15.46	–	~700
11	L	F11 (5–8)6	61.2	dark	canc.	–	B	3.83	0.01	37.9	17.99	28; 44	600–700
11	L	F11 (5–8)6	62.1	dark	cort.	8.11	B	3.88	0.01	38.41	18.04	–	600–700
11	L	F11 (5–8)6	63.1	dark	cort.	5.16	A	5.52	0.64	36.68	18.08	–	800–900
11	I	F11 (1–2)1	28.1	light	cort.	1.36	D	4.59	1.15	34.90	*	28; 44; 91	~700
11	I	F11 (1–2)1	28.2	light	cort.	–	D	4.81	0.89	33.84	15.07	–	700–800
11	I	F11 (1–2)1	30.1 white	light	cort.	–	C	6.27	–	40.11	19.67	–	~900
4	D	F4.D02	32.1	light	canc.	1.09	C	6.33	0.70	36.19	17.79	–	600–700
5	J	F5.H301	34.1	light	cort.	2.06	C	5.52	0.90	29.50	14.55	–	600–700
8	A	F8.A0	36.1	light	canc.	2.38	D	5.31	0.87	40.26	15.63	–	~700
11	L	F11 (5–8)6	66.1	light	cort.	–	B	3.69	0.18	39.89	19.55	28; 44	500–600
11	L	F11 (5–8)6	66.2	light	canc.	0.83	D	4.29	0.80	40.08	19.52	28; 44	600–700

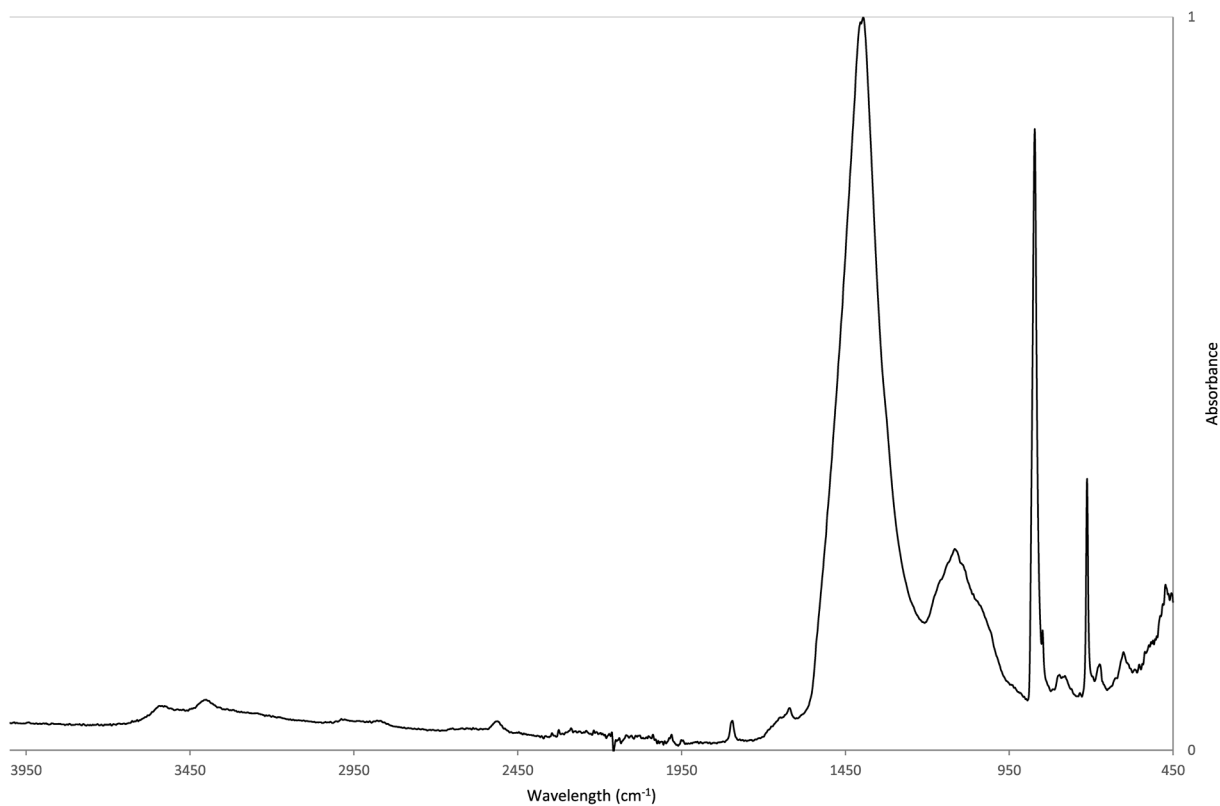


Fig. 6. FTIR spectrum of limestone from Abri Pataud.

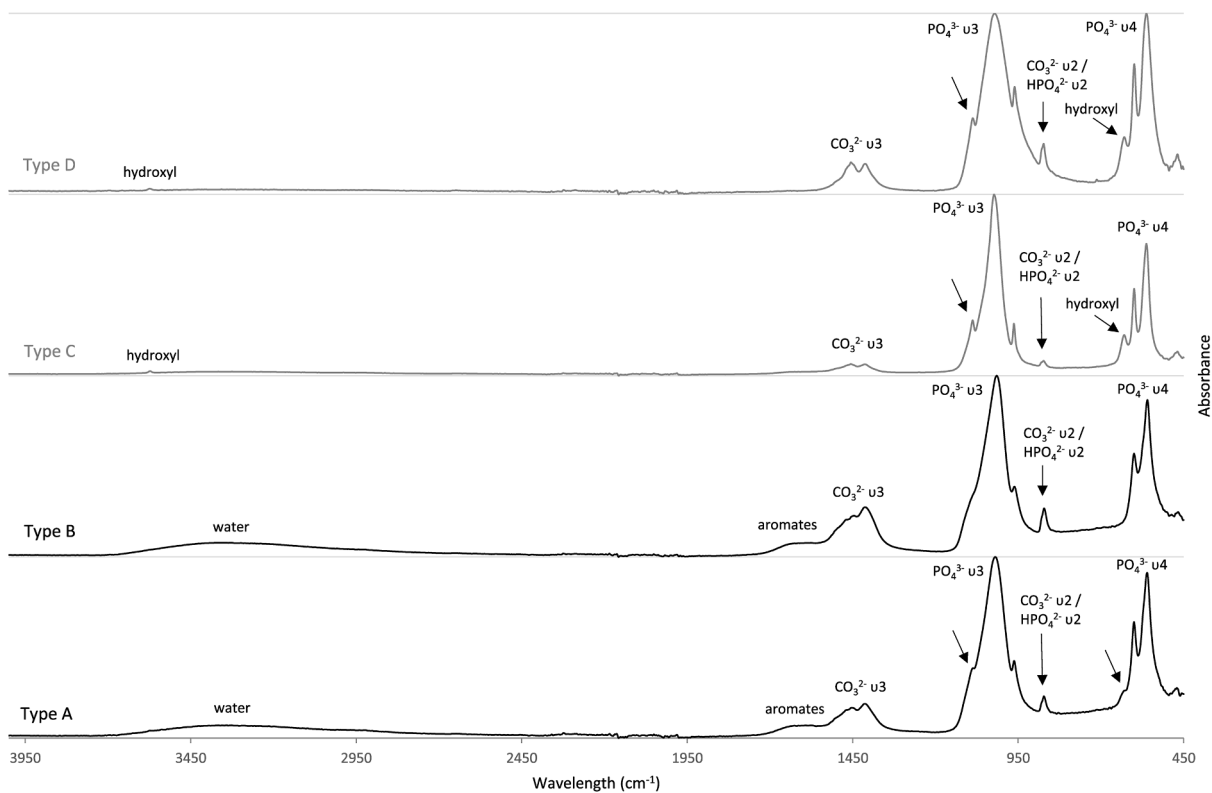


Fig. 7. FTIR spectra representative of the four types of heated bone samples found at Abri Pataud, with the most notable peaks labelled or indicated with an arrow in case of tentative identifications. Type A and B (black) refer to dark coloured samples. Type C and D (grey) refer to light coloured samples.

fragments of (alkyl)benzenes ( $m/z$  91 and 78).

4.2. Microscopic heat altered materials

4.2.1. Polymorphs of silica ( $SiO_2$ )

Three distinctive groups of polymorphs of silica were observed in the samples (Fig. 8). (i) Amorphous opal or phytoliths, mostly ill-defined (Fig. 8a). (ii) Microcrystalline material or chalcedony, which can

be qualified in this context as flint chips, the small waste of flint knapping activities at the site (Fig. 8b). (iii) Crystalline quartz grains, interpreted as sediment particles.

4.2.2. Calcium oxalate crystals and spherulites

In the samples typical heated oxalate crystals are present, transformed into calcium carbonate, but keeping their original crystal form (Brochier and Thinon, 1993) (Fig. 9). Dung spherulites were not

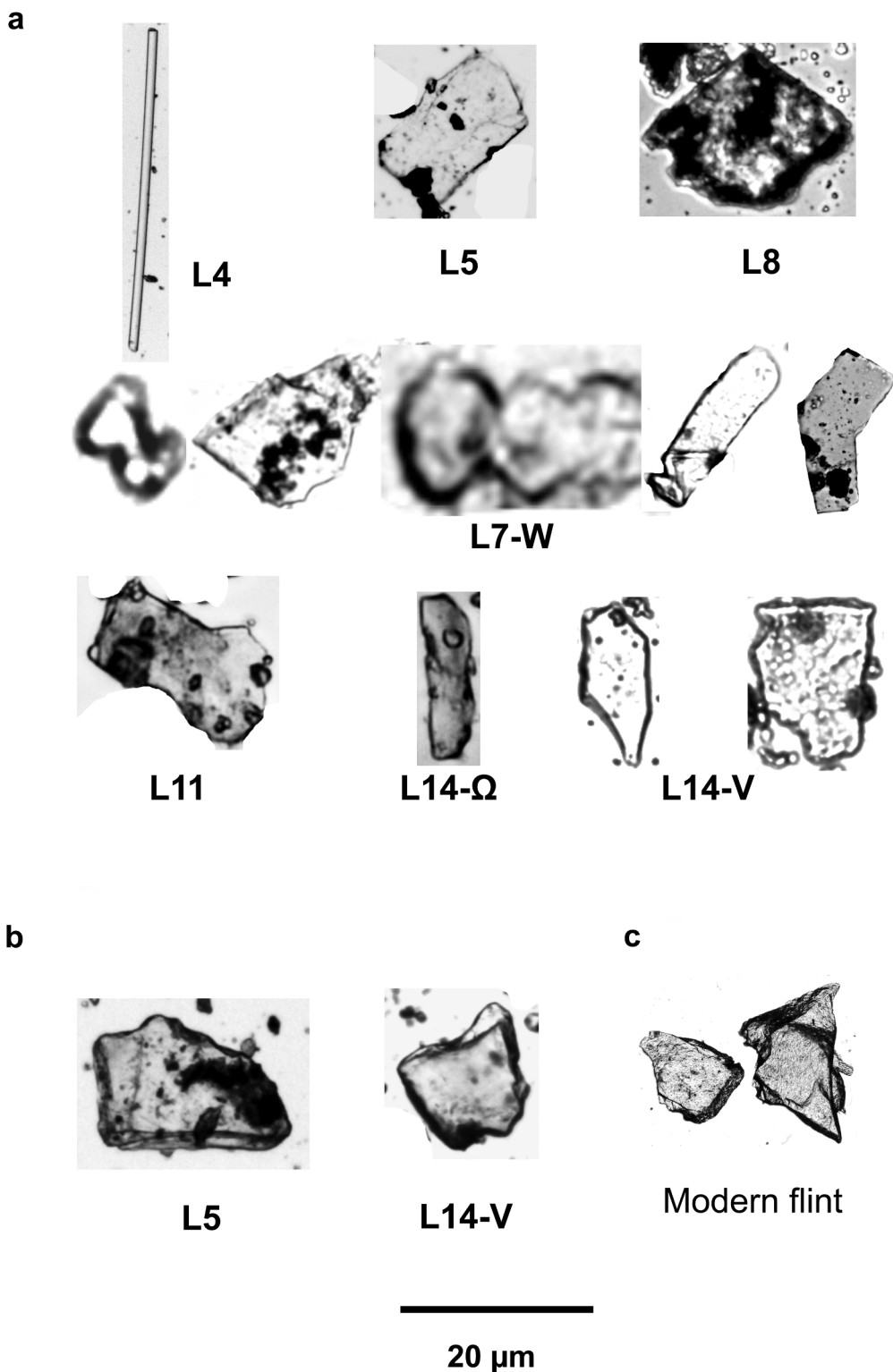
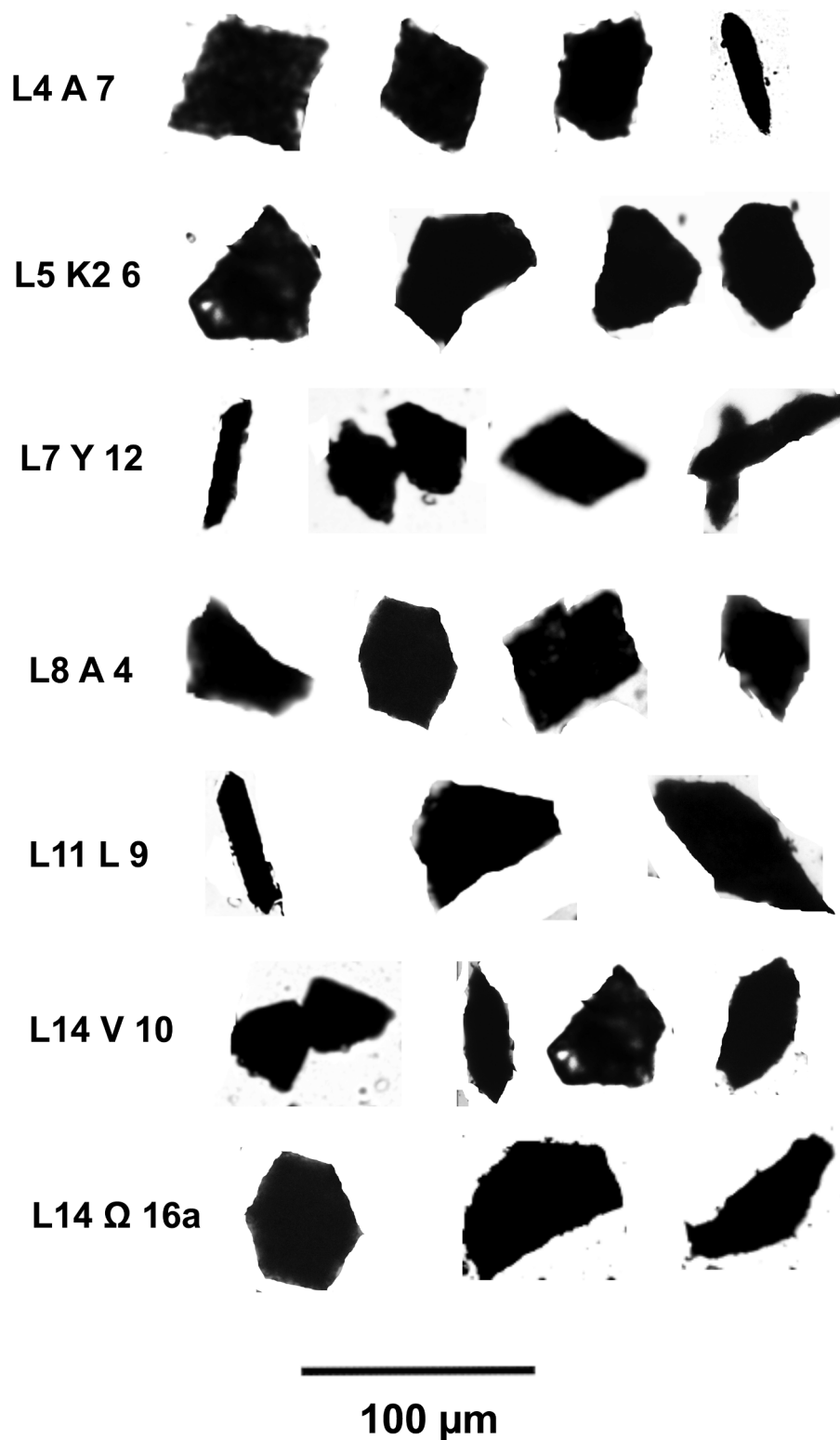


Fig. 8. Silicate polymorphs. (a) ill-defined phytoliths, b) flint flakes from hearths and (c) modern flint flakes.



**Fig. 9.** Dark micritic calcite pseudomorphs after calcium oxalate (POCC) recovered from the Abri Pataud museum glass jars (4-16a) sampling the infill from the indicated archaeological levels (L4-L14) and hearths (A-Ω).

observed in the samples.

#### 4.3. Sediment matrix (< 200 μm)

##### 4.3.1. Sediment pH

The pH of the recently obtained sediment samples from Levels 4 and 11 is 8.2 and 9.9, respectively. In addition, the sediment sample

obtained from Level 2 has a pH of 8.9. The pH of samples from the fill, taken by Movius and stored in the glass jars, ranges from 8.3 to 8.9 (Table 6).

##### 4.3.2. Analytical pyrolysis: Macromolecules in sediment

The chromatograms show that in the fills of the hearths five classes of compounds are present (Supplementary Table 1a for Py-GC-MS

**Table 6**  
pH measurements on sediment and fill samples, including limestone fragments from the Abri Pataud.

Level	Sample	pH
2	Sediment	8.9
4	Sediment	8.2
11	Sediment	9.9
4	Fill, jar 6	8.9
7	Fill, jar 4	8.9
11	Fill, jar 11	8.6
12	Fill, jar 3	8.3
14	Fill, jar 16a	8.3
-	Limestone	8.3

products, and [Supplementary Table 1b](#) for THM products).

The combination of HF-treatment and the use of a resistive heating pyrolyser (which allows for relatively large sample amounts) resulted in the detection of numerous pyrolysis and THM products that allowed for the identification of various sources of organic matter.

Firstly, all samples produced benzene, toluene and series of polycyclic aromatic hydrocarbons (PAHs) such as naphthalene, methyl-naphthalenes, biphenyl, fluorene and anthracene/phenanthrene, with Py-GC-MS. Together with compounds such as dibenzofuran and benzonitrile, this series of compounds is indicative of the presence of COM (Kaal et al., 2008; Fabbri et al., 2012a). With THM-GC-MS, the COM can be recognised from the presence of the same PAHs (mostly naphthalenes and fluorene), in addition to benzophenone and a series of benzene carboxylic acids (BCAs, detected as methyl esters). The BCAs include benzoic acid methyl ester, but also benzene dicarboxylic acid dimethyl ester and the tri- and tetracarboxylic analogues. Especially the BCAs with three and four carboxylic groups are not common products of lignin and are very likely the products of oxidised COM (Kaal and Filley, 2016).

A second series of products, which contain nitrogen, can be ascribed to the remains of bone or meat collagen. This is the case for the typical series of pyrrole and diketodipyrrole with Py-GC-MS (Chiavari and Galletti, 1992; Adamiano, 2012; Cersoy et al., 2018). Especially the strong dominance of pyrrole over pyridine discards pyrogenic N moieties or non-collagenous protein as the main source of the N-compounds in the samples with a clear collagen fingerprint (Kaal et al., 2016). In the samples with a significant collagen content, the toluene is also largely associated with collagen, and not COM (both are prolific of this compound). Furthermore, several samples provided clear signals of charred N moieties, represented by compounds such as pyrrole carbonitrile, pyridine carbonitrile, (iso)quinoline and indoleione. These compounds indicate the presence of COM from a N-rich source such as collagen (Kaal et al., 2008). In samples with high proportions of indicators of charred N groups, an unknown fraction of the toluene and PAHs probably originates from charred collagen as well. Because the THM fingerprints of charred collagen have not been described in detail in the literature, the THM data cannot be linked to the presence of these constituents. However, preliminary experiments using amino acids and oligopeptides showed that proline produces a series of compounds with

$m/z$  108 and 139, and  $m/z$  108 and 138, among several other more ubiquitous products such as C<sub>4</sub>- and C<sub>5</sub>-alkylpyrrole and an unidentified compound with base ion  $m/z$  98 (including N-methylproline methyl ester) (Hendrickler and Voorhees, 1998; Knicker et al., 2001). These compounds were detectable in the THM fingerprints studied, which is probably an indication of the presence of proline-rich proteins in the samples, such as collagen. In this sense, the detection of a N-methylphthalimide (probably the methylation product of the indoleione detected with Py-GC-MS), may be indicative of N-containing COM (e.g. charred collagen) upon THM.

Other identified Py-GC-MS products are phenols, which may originate from any source, and a series of cyclopentenones and furans, which are indicative of polysaccharides. The lack of anhydrosugars and other typical products of plant-derived polysaccharides suggests that these compounds originate from microbially or thermally altered polysaccharides, of which the latter is the more likely explanation considering the evidence of COM in all samples (Braadbaart et al., 2004). The presence of these peaks suggests that some of the COM originates from lignocellulose feedstock. With THM the carbohydrate component is poorly observed, but a minor peak of derivatised glucopyranoside is in agreement with the presence of such materials (Fabbri and Helleur, 1999). This peak was most pronounced in sample L11 (subsample taken next to the hearth), which was also the only sample with a possible lignin signature (methylation products of *p*-coumaric acid and other products such as 3,4- di- and 3,4,5-trimethoxy benzoic acid, methyl ester). Hence, recognisable (uncharred or weakly charred) plant remains are preserved to some extent in the sediment.

Finally, a series of alkenes/alkanes and fatty acids (or fatty acid methyl esters with THM) can be observed, which may originate from food residues or other sources that contain lipids. The presence of alkylnitriles (C<sub>16</sub> and C<sub>18</sub>) are likely pyrolysis products of fatty acid in the presence of N (Evans et al., 1985; Nierop and Van Bergen, 2002), and typical of meat fat, but also of many other sources. From meat charred at 310 °C typical protein-derived products such as toluene, styrene, phenol, the methylphenols and diketopiperazines (Fabbri et al., 2012b) were released along with C<sub>16</sub> and C<sub>18</sub> amides, the intermediates between fatty acids and fatty nitriles. At 400 °C, all these compounds were hardly detectable, with the exception of toluene. Instead, relatively small, but distinct peaks of a homologous series of *n*-alkenes/*n*-alkanes appeared. Most likely these products were derived from the fatty acids which were either polymerised over time to produce aliphatic macromolecules (e.g. Versteegh et al., 2001) or as fatty acids bound to minerals or salts (Hartgers et al., 1995). In all hearths these *n*-alkenes/*n*-alkanes range from C<sub>7</sub>-C<sub>16</sub> or C<sub>18</sub>, of which the maximum chain length confirms such a fatty acid origin.

In summary, the Py-GC-MS and THM-GC-MS results of the sediment materials are indicative of the presence of 1) collagen, which is derived from bones and or meat, 2) charred organic matter, which corresponds to charred collagen and other charred remains (from fuel e.g.), the relative proportions of which cannot be determined, 3) traces of recognizable lignocellulose (L8 and L11) and 4) lipid-derived materials the source of which cannot be elucidated with the available data. It is worth noticing that this study represents a very explicit identification

**Table 7**

Ancient mammalian families identified by their DNA in sediment samples collected from fireplaces at Abri Pataud. Layers, glass jar number and hearth labels are indicated, but for one sample from Layer 5 ("adjacent area"), from the Layer 5 matrix.

Layer	Jar	Hearth	Bovidae	Canidae	Cervidae	Equidae	Hominidae
L4	#6	A					
L5	#9	H-3 subdivision		+			
L7	#5	W-2					
L11	#35	N		+		+	+
L12	#3	P	+	+	+	+	+
L14	#16a	Ω		+	+		+
L5	Adjacent area	Matrix L5		+			



of collagen in sediment organic matter on the molecular level using analytical pyrolysis techniques. Hitherto, collagen fingerprinting had been performed mainly in collagen extracts or animal glue isolates (e.g. Chiavari and Galletti, 1992; Orsini et al., 2017), with the exception of Kaal et al. (2019), who observed collagen-dominated pyrolysates in samples from a Neolithic elk processing site in Sweden.

#### 4.4. DNA analysis

The number of library molecules generated from the artificial oligonucleotide spiked-into the library preparation was at least one order of magnitude lower in the sample libraries than in the associated negative controls (Supplementary Table 2). This suggests that inhibitory

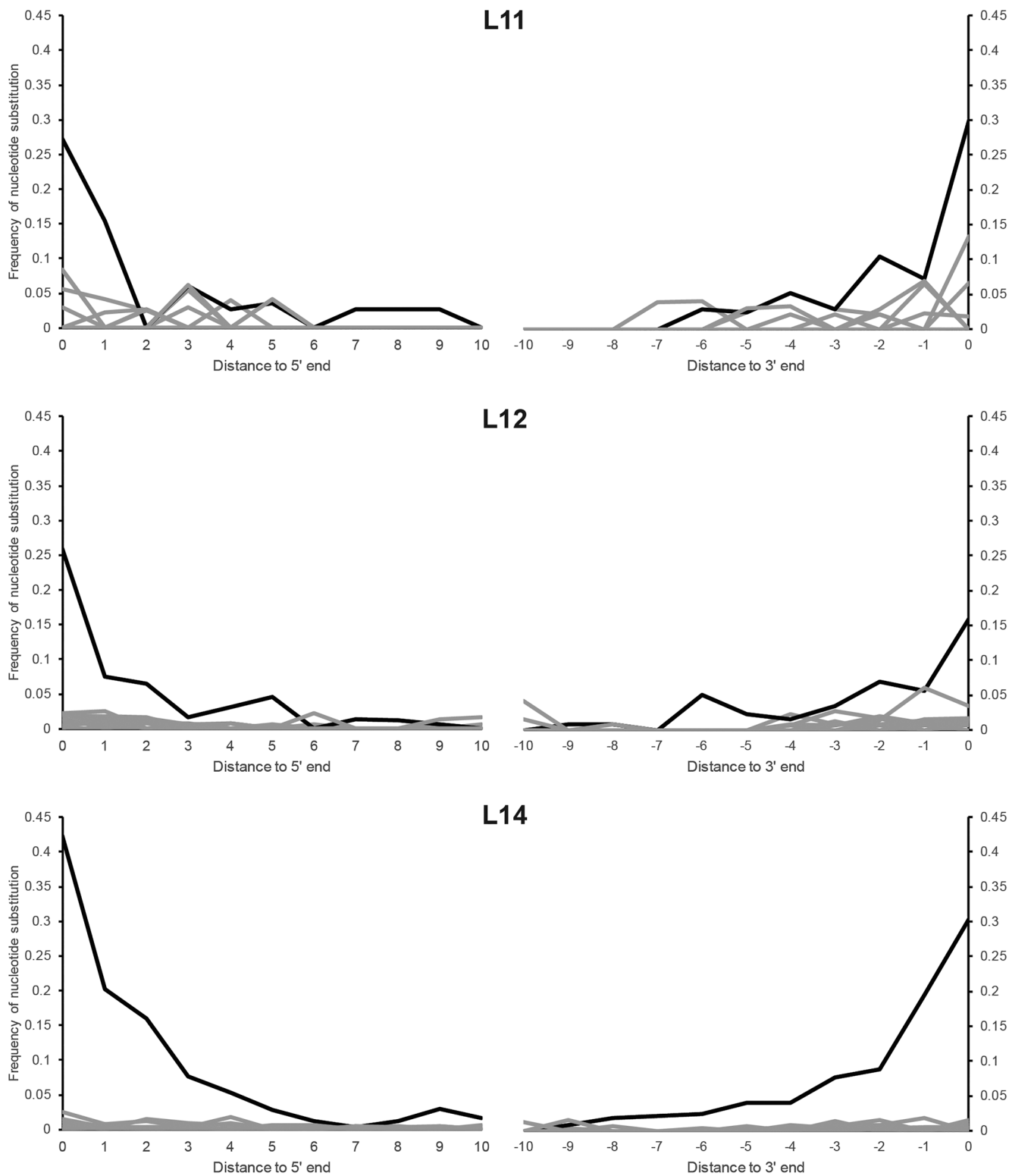


**Fig. 10.** Patterns of DNA damage in the hominin mtDNA fragments yielded from sediments deposited in layers L11, L12 and L14. Elevated frequencies of cytosine to thymine nucleotide substitutions (black lines) towards the beginning and end of fragments are indicative of the presence of ancient DNA in a sample. All other substitution types are marked in gray.

substances were co-extracted with the DNA from the sediment samples, hindering the full conversion of DNA fragments into DNA library molecules (Glocke and Meyer, 2017). Nonetheless, we were able to detect ancient mammalian mtDNA fragments in five of the seven samples tested. None of the negative controls contained evidence for the presence of ancient DNA.

In the five positive samples, faunal mtDNA fragments with evidence for ancient DNA base damage originated from Bovidae, Canidae, Cervidae or Equidae, coinciding with faunal remains found at the site (Bouchud, 1975). Three of the samples also contained ancient hominin mtDNA (Table 7, Fig. 10). Of these, we recovered too few ancient hominin mtDNA fragments in the samples from layers L11 and L12 to determine a hominin group of origin. From the sample collected in Early Aurignacian level L14, we recovered 165 hominin mtDNA fragments displaying signs of ancient DNA damage. All damaged fragments that overlapped positions diagnostic for modern human mtDNA matched the modern human variant (4/4 fragments), while none matched the Neandertal, Denisovan or Sima de los Huesos variants at diagnostic positions for these groups (0/7, 0/15 and 0/17 fragments, respectively) (Supplementary Table 2). This suggests that the ancient mtDNA fragments recovered from sediment deposited in layer L14 originated from one or more modern human-like mitochondrial genome(s).

## 5. Discussion

### 5.1. Introduction

At the onset of this study we inferred that combining the results of laboratory experiments with those of multi-proxy studies of the contents of the hearths from Abri Pataud might provide reliable information about the function of former fires and changes in fire-related activities through time. The focus of this study was on the fuel type(s) used by the site's occupants, the temperatures reached in fireplaces, the potential changes in human activities related to fireplaces over time, with the influence of post-depositional processes taken into explicit consideration. We will discuss the results from this multi-proxy study against the background of these questions.

### 5.2. The effect of pH

Abri Pataud represents an alkaline depositional environment, with all analysed sediments and hearth fills having a pH that exceeds 8 (sediments: 8.2 – 9.9; hearth fills: 8.3 – 8.9). The high pH of the site is likely the result of weathering of the limestone rock shelter wall (pH 8.3), and the deposition of ashes (pH 9–13: Etiegni and Campbell, 1991), resulting in carbonate-rich and ashy sediments (Marquer, 2010). This also explains why the pH is relatively constant throughout the sequence, spanning a period of roughly 20,000 years. Alkaline conditions affect heated materials in a variety of ways. An earlier laboratory investigation with charcoal samples incubated in an alkaline environment showed that deposition under these conditions results in increased solubility of the aromatic compounds and strong fragmentation, which may lead to a loss of up to 50 wt% of charred material. In addition, this chemically-mediated micro-fragmentation causes a decrease in the reflective properties of the char, resulting in lower %R<sub>0</sub> values and related heating temperature reconstructions (Braadbaart et al., 2009). Complementary experimental research on the effect of pH on heated bone shows that alkaline conditions have a similar effect on charred collagen (Reidsma, in prep), resulting in partial dissolution, fragmentation, and loss of organic compounds. Furthermore, high pH values do not just have an effect on organic compounds, but can also impact inorganic materials. For example, it has been shown that phytolith preservation is affected in alkaline environments (Canti and Huisman, 2015; Xiao et al., 2001). This involves deprotonation of the Si-OH groups, which opens up the Si-O-Si bonds of the phytoliths to nucleophilic attack of OH<sup>-</sup> ions in water, resulting in the dissolution/release of Si (Nguyen

et al., 2014).

The effect of the alkaline depositional environment at Abri Pataud is clearly visible in the various fire proxies. Most clearly affected are the charred plant remains (COM), which display highly fragmented structures. The high degree of fragmentation of the charcoal was also observed in an earlier study by Marquer et al. (2010). Their quantification study of COM showed that charcoal mainly preserved at the micro-scale while charred bones were still abundant at macro-scale. Comparable results were obtained in studies of other archaeological contexts (Marquer, 2010; Marquer et al., 2012). pH-mediated fragmentation of chars would therefore explain the scarcity of macroremains and the over-representation of heated bone fragments at Abri Pataud, alongside the role of mechanical fragmentation processes (Chrzavzez et al., 2014). Further confirmation of the effect of alkaline conditions on the COM can be found in the FTIR results, which are most similar to reference data on charcoal exposed to alkaline solutions (pH 12). The heated bone tissue at Abri Pataud appears to be affected differently. FTIR shows incorporation of exogenous carbonates (originating from the limestone of the rock shelter), which makes it difficult to assess the effect the alkaline environment had on the organic content of the bones. However, the incorporation of exogenous carbonates likely resulted in the underestimation of the relative percentage of organic content based on TGA, resulting in possible overestimation of the heating temperature for those results. Additionally, preliminary experimental results show that alkaline conditions may result in increased crystallinity of heated bones, causing possible overestimation of heating temperatures based on SF and CI values (Reidsma, in prep.). Our results suggest that the phytoliths found at Abri Pataud are also affected by the site's alkaline conditions. Most of the phytoliths are characterised by ill-defined morphotypes, which is likely the result of partial dissolution. Finally, it should be considered that pH-mediated dissolution of heated and unheated organic compounds may have contributed to the bio-molecular signatures in the sediments at Abri Pataud, even though at least some of the sediment samples showed excellent preservation of the collagen's molecular fingerprints. In order to correct for the effect of alkaline conditions we have incorporated reference data on the effect of high pH in our reconstructions of heating conditions based on the affected materials. This reference data consists of extensive experimental work conducted by the authors (Braadbaart et al., 2009; Reidsma, in prep.).

### 5.3. Fuel use

As shown by the charcoal structure of most of the samples (Fig. 3 a, b, c, d, e and f), together with the calcium oxalate crystals (Fig. 9) found in all the investigated hearths, woody plant material must have been used as the major fuel resource during Aurignacian and Gravettian occupation of the site. However, in hearths in Early Aurignacian levels L11 and L14, samples of COM material, based on their structure, are not derived from wood (Fig. 3 g), but rather from (lignin-containing) fibrous/grassy plant material, very probably dung. As far as we know, this is the earliest reported use of dung as fuel. Our interpretation could not be confirmed by unambiguous identification of spherulites in the samples, possibly because their preservation would be exceptional in samples of such high age and high alkalinity (pers. comm. J.E. Brochier to F.B. 2018) or because the diet of the ruminants did not favour the formation of spherulites (Smith et al., 2019). Considering the large amount of reindeer bones recovered at the site (Bouchud, 1975; Cho, 1998; Crepin, 2013; Sekhr, 1998; Vannoorenberghe, 2004) reindeer excrements must have been readily available in the landscape. Ethnographic data show that in subarctic areas of Asia and North America reindeer dung was a very important – and sometimes the only – fuel source (e.g. Zgusta, 2015). Compared to wood, dung and peat are much more efficient fuels (Braadbaart et al., 2012). Use of dung may have been a strategy to deal with decreased wood availability. Apart from variations in their availability – and hence varying cost/benefits of these fuel types (cf. Henry et al., 2018) – the different heating qualities

of these materials (Braadbaart et al., 2012) were probably used as a tool to adjust fire conditions to specific needs.

Many bone fragments were recovered from the excavated hearths, as has been observed at other Upper Palaeolithic sites too (e.g. White et al., 2017). Their presence in fireplaces is generally interpreted as indicative of the use of bone as fuel, possibly related to i) the scarcity of dry standing wood in the steppe-like environments of glacial Europe (Vidal-Matutano et al., 2017; Théry-Parisot et al., 2018), ii) specific activities related to the fireplaces and/or iii) resulting from taphonomic issues (e.g. Théry-Parisot 2001, 2002; Villa et al., 2002; Costamagno et al., 2005; Théry-Parisot et al., 2005, 2010; Marquer et al., 2010, 2012; Chrzavzez et al., 2014). However, it is unlikely that this material was primarily used as fuel, as bone tissue consists of 70 wt% inorganic material: it is the organic material that carries the energy that can be transformed into heat and for bone tissue only about 20 wt% is organic collagen. The high ash content thus reduces the heating capacity considerably, to less than 4 MJ kg<sup>-1</sup> (daf) compared to the ~19 MJ kg<sup>-1</sup> (daf) for collagen and other common fuel types like wood (calorific values for bone calculated on basis of average wood values, e.g.: Günther et al., 2012). In this study bone tissue refers specifically to the rigid part of the bone, while possibly attached lipids like fat and marrow are not considered. Bone tissue as defined here also lacks the open structure of wood and other fuels and as a result there is limited access for air through the dense cortical bone to the charred collagen part. In turn this carbon-containing part will not easily burn or combust and as a result generate heat. In addition, the collagen is very finely dispersed within the bone tissue. These considerations render bone unsuitable as a fuel; this topic is extensively discussed in Reidsma et al. (2016).

Furthermore, among the bone fragments recovered from the Abri Pataud hearths, 70% is dark-coloured dense cortical bone, while less than 30% consists of light-coloured and spongy cancellous bone (Table 5). Often the light-coloured outside of the heated bone tissue has an inner part that remained dark-coloured. Hence, the majority of the bones from the Abri Pataud fireplaces were not *combusted* but *charred*, and therefore likely heated indirectly, i.e. not used as fuel. The abundance of bones in a hearth can also result from post-depositional processes that better preserve heated bone materials than charred plant material (Marquer et al., 2010, 2012), especially with high sediment pH.

Finally, bone contains marrow and fat, which are comprised of lipid biomolecules and therefore excellent fuels. However, these lipids are also generally considered to have been a very important food source for Pleistocene hominins (Speth, 2010), implying that the use of lipids for either fuel or food minimally required careful consideration of the local resource landscape. As White et al. (2017) have put it, "...an overly high dependence on bone as fuel would result in the improbable situation of humans hunting to feed the fire" (2017: p. S298).

Our views on the limited suitability of bone as fuel find some support in the results of a recent cross-cultural survey of on-site fire use by ethnographically documented hunter-gatherers (McCauley et al., 2020, in press). In a sample of 93 hunter-gatherer groups, that, importantly, included groups in the Arctic, these authors did not find any evidence of the use of bone as a fuel source. They stated that this is "intriguing because it has been argued that bone was utilized for fuel in Palaeolithic Europe" (McCauley et al., 2020 in press). For the reasons given above we suggest that bone was not a suitable fuel and that hence the hypothesis of a widespread use of bone as fuel in the Pleistocene must be considered with caution.

#### 5.4. Heating conditions: Temperature and oxygen availability

##### 5.4.1. COM

The FTIR spectra of the eight COM samples show three main bands at 3400, 1558 and 1385 cm<sup>-1</sup>, corresponding most closely to the morphology and intensity of the bands present in modern charcoal

subjected to an alkaline solution (Fig. 4). Nevertheless, it should be noted that the COM samples from Abri Pataud show more similarity to other archaeological material, than to the modern reference data. It is therefore difficult to give a very precise temperature estimate. Temperatures may range between 340 and 600 °C, but likely fall at the lower end of this range (between 340 and 400 °C). These results match well with the reflectance measurements of the COM samples, which show that temperatures between 350 and 450 °C were reached (Table 3).

##### 5.4.2. Bone tissue

For the various dark-coloured bone tissue samples excavated from the Abri Pataud, two types can be distinguished based on the form and intensity of the FTIR spectra, which are in good agreement with the results of the laboratory experiments on modern charred bone (Reidsma et al., 2016). This is further supported by the TGA results, which show that some of the organic carbon is still present. A broader comparison of the results of the dark-coloured bone samples with the charred bone reference data suggests heating temperatures between 500 and 900 °C (Table 5).

For the lighter-coloured archaeological samples two types can also be distinguished based on the form and intensity the FTIR spectra. These spectra are most similar to spectra obtained in laboratory experiments with modern combusted bone (van Hoesel et al., 2019). Especially the presence of hydroxyl bands confirms heating in the presence of air. TGA results again comply with these conclusions since the organic carbon content ranges around 1.7 wt% meaning that most carbon oxidised. Comparison with the combusted bone reference data suggests the light-coloured bone samples were heated to temperatures between 500 and 900 °C (Table 6).

The large proportion of charred bone tissue (70%) related to the hearths at Abri Pataud suggests that the material was heated indirectly. The proportion of combusted material shows that when bone was heated directly, they registered relatively high temperatures in the fires (the same is true for the material heated indirectly). This is in contrast with the much lower temperatures registered for the COM. However, this should not be surprising as organic materials heated in the presence of oxygen will oxidise at temperatures above 300 °C and burn until only ash is left. Char will therefore only survive if the fuel is deprived of oxygen or if the temperature drops below the threshold temperature, resulting in a likely underestimation of the temperatures reached in the fire. The presence of large quantities of ash at Abri Pataud confirm that oxidation of organic fuels took place and temperatures attained in the fires were higher than 400–450 °C. Our results thus show that combining different fire proxies provides a more complete picture of the use of a fire, in terms of temperature as well as oxygen availability.

#### 5.5. Fire functions (and changes over time)

The macroscopic, microscopic and molecular artefacts from and around the hearths in the sequence of the fourteen archaeological levels in the Abri Pataud show interesting differences through time, which may provide further insights in the function of the hearths and in the behaviour of the occupants of the rock shelter. In the Early Aurignacian levels heated river pebbles are very low in numbers or sometimes not present at all, while they are common to abundant in the Evolved Aurignacian and Gravettian levels. Simultaneously the temperature of the recovered COM material increased gradually during these periods of time from 350 °C in the Early Aurignacian to 450 °C in the Gravettian. The so-called bonfires, large spreads of ashy material, are only found in the Gravettian. Interestingly, the Py-GC-MS chromatograms showed that in the older levels polysaccharide-derived furans were not present, which might indicate that the function of the fires as well as specifics of the fueling and/or cooking process may have changed over time, i.e. that the Early Aurignacian occupants of the rock shelter used the generated heat in a different way than the Gravettian ones. We cannot

assess the influence of the higher age of the Aurignacian assemblages here, but given that pH values are the same throughout the entire sequence, these differences between the Aurignacian and Gravettian levels can tentatively be ascribed to differences in behaviour. This supports the results of Marquer et al. (2010), who statistically discriminated Early Aurignacian, Evolved Aurignacian and Gravettian samples based on analyses of microscopic charcoal and charred bones. Long-term changes in local temperature and humidity may have been one of the factors determining these behavioural changes, as there is some evidence that the period over which the Gravettian layers formed was somewhat less cold and more humid than during the deposition of the Aurignacian find levels (Lenoble and Agsous, 2012; Marquer et al., 2010). One could suggest that for the Aurignacian occupants of the site, animal products (“meat”) constituted a more important food resource than for later occupants, as no furans were recognised in Aurignacian fireplaces. Alternatively, the absence of furans from the Aurignacian levels may point toward different fuel use, or processing of plant materials in a different manner than the Gravettian occupants did. While all studied fireplaces were situated within the rock shelter, it may be possible that part of the changes described here were also related to changes in the morphology of the *abri* during the Aurignacian and the Gravettian, but it is impossible to assess which ones and to which degree.

### 5.6. Fire authorship

The ancient mtDNA fragments recovered from sediment deposited in the Early Aurignacian level L14 originated from one or more modern human-like mitochondrial genome(s). To our knowledge, this makes Abri Pataud the first archaeological site for which modern human mtDNA has been retrieved from sediment samples.

The detection of ancient mammalian mtDNA fragments in sediment samples from the Abri Pataud fireplaces as well as from a control sample coming from outside of a fireplace calls for a follow-up study to achieve a better understanding of the taphonomy of these biomolecules within the Abri Pataud sequence. It is possible for DNA to survive exposure to high temperatures (Sawyer et al., 2012), even as high as 1000 °C (Klein et al., 2018). Did these mtDNA fragments indeed survive exposure to temperatures registered by the COM (350–450 °C) or bone tissue (500–900 °C), and are they (partially) the result of food preparation practices? Or is their presence in the Abri Pataud fireplace’s infill (also) a post-sedimentary phenomenon? Study of samples taken systematically all through the site’s stratigraphy could yield data to answer questions regarding these (not necessarily mutually exclusive) scenarios.

## 6. Conclusions

The current study aimed to apply an integrated approach to improve our knowledge about fire-related behaviour of the Aurignacian and Gravettian occupants of the Abri Pataud. For this purpose the physical and chemical properties of macroscopically visible as well as ‘invisible’ artefacts recovered from archaeological excavations of the infill of Upper Palaeolithic fireplaces were explored. Specific attention was paid to fuel use, the reconstruction of past heating conditions, fire functions, and changes in human activities over time, while the effect of diagenesis was taken into account. Based on this research the following conclusions can be drawn:

(a) The limestone environment of the hearths and their fills at this site are highly alkaline, which has had its effects on the properties of the investigated heated materials. The properties of the affected materials appear to correspond to modern reference materials that were incubated in alkaline solutions, suggesting that the results of such experiments can be used for archaeological research. Results also suggest that accounting for diagenetic effects is necessary.

- (b) As fuel, charred organic material was identified, including charcoal and charred dung, probably from reindeer. To our knowledge this is the earliest reported use of dung as fuel. Calcium oxalate crystals and phytoliths recovered from the ash showed that plant material was used as fuel in all levels. While heated bone was abundant, earlier suggestions about the use of bone tissue as fuel are not supported by this study: our analyses indicate that bone tissue was not a suitable fuel during the Palaeolithic, not even in periods with limited availability of dry standing wood.
- (c) The discrepancy between the reconstructed past heating temperatures based on charred organic material (350–450 °C) and those based on the heated bone tissue (500–900 °C) and abundance of ash (greater than 450 °C) suggests that 1) charred organic material likely underestimates past heating temperatures due to the nature of its formation and preservation, and that 2) integrating different fire proxies provides a more complete picture of past heating conditions.
- (d) In addition, the difference between charred and combusted bone tissue could be determined. The results show that in all levels ~70 wt% of the bone fragments was charred and less than ~30 wt% was combusted. This suggests a high rate of indirect heating of bone fragments, challenging previous assumptions about the use of bone as a fuel at Abri Pataud.
- (e) Next to macroscopically visible artefacts, ‘invisible’ artefacts were present as well. Microscopic work on the hearth fills resulted in the identification of the following polymorphs of silica: phytoliths, microscopically small flint flakes and quartz crystals. Calcium oxalates were found in abundance. Faecal spherulites were not preserved in the investigated samples.
- (f) A second category of ‘invisible’ artefacts recovered from the hearth fills consists of molecular biomarkers. In the Abri Pataud five classes of compounds were shown to be preserved despite the degrading processes normally occurring in sediments: polysaccharides and lignin derived from plant material, N-containing aromatics related to the heating of animal protein (collagen in bone and/or meat), PAHs from charred organic material, and alkenes/alkanes and fatty nitriles, both from lipids. This includes explicit identification of collagen in sediment organic matter on the molecular level using analytical pyrolysis techniques.
- (g) Interesting differences in the presence of specific heat-altered materials were found between the various archaeological levels, suggesting that fire-generated heat was used in different ways. For instance, in contrast to the Gravettian occupation layers, in the Aurignacian levels both furans as well as heated river pebbles were largely absent. Differences in heating temperature (based on COM) were also observed between the two periods. Nevertheless, more research is needed to get to clearer interpretations of fire function.
- (h) The detection of ancient mammalian mtDNA fragments in sediment samples from the fireplaces, as well as from a control sample outside of a fireplace, calls for a follow-up study to achieve a better understanding of the taphonomy of these biomolecules within the Abri Pataud sequence. The ancient mtDNA fragments from one or more modern human-like mitochondrial genome(s) recovered from sediment deposited in the Early Aurignacian layer L14 make the Abri Pataud the first archaeological site for which ancient modern human mtDNA has been retrieved from sediment samples.
- (i) Our results show that an integrated approach, combining different fire proxies and different analytical techniques and explicitly accounting for diagenesis, is required to obtain a more complete picture of the use of fire.
- (j) The results obtained from the sediment samples taken by the Movius team more than half a century ago suggest that systematic sampling of fireplaces and their sedimentary matrix should become a standard part of the excavation protocol of such features, and that analysing samples taken during older excavation campaigns can still prove very fruitful.

## Acknowledgements

We are grateful to the late Hallam L. Movius Jr and his team, for the care with which they documented and sampled the infill of fire-related features at the Abri Pataud, more than half a century ago, without which this study would not have been feasible. Our project was funded by the Koninklijke Nederlandse Akademie van Wetenschappen (knaw.nl), Academy Professor Prize program 2013, awarded to Wil Roebroeks. Technical assistance with the reflectance measurements by Harry Veld of Deltares (Utrecht, the Netherlands) and of Eric Mulder (Faculty of Archaeology, Leiden University) and Ton van Brussel (Institute of Biology Leiden, Leiden University) with the phytolith research are greatly acknowledged. We would like to thank the following people from the Dutch Cultural Heritage Agency (RCE) for their help with the measurements: Suzan de Groot for assistance with the FTIR and Henk van Keulen for his assistance with the PyMS. Sophie Jorgensen-Rideout gave helpful comments on an earlier draft of the manuscript. The genetic work was funded by the Max Planck Society and the European Research Council (grant no. 694707 to Svante Pääbo). We thank B. Nickel, J. Richter, B. Schellbach and A. Weihmann for work in the ancient DNA laboratory of the Max Planck Institute for Evolutionary Anthropology at Leipzig. The sequencing data generated for the ancient DNA project were deposited in the European Nucleotide Archive under accession number PRJEB31258.

## Appendix A. Supplementary data

Supplementary data to this article can be found online at <https://doi.org/10.1016/j.jasrep.2020.102468>.

## References

- Aarts, J.M.M.J.G., Alink, G.M., Scherjon, F., MacDonald, K., Smith, A.C., Nijveen, H., Roebroeks, W., 2016. Fire usage and ancient hominin detoxification genes: protective ancestral variants dominate while additional derived risk variants appear in modern humans. *PLoS ONE* 11, e0161102.
- Adamiano, A., 2012. Pyrolysis of peptides and proteins. Analytical study and environmental applications. PhD Thesis, Università di Bologna DOI 10.6092/unibo/amsdottorato/4671.
- Adamiano, A., Fabbri, D., Falini, G., Belcastro, M.G., 2013. A complementary approach using analytical pyrolysis to evaluate collagen degradation and mineral fossilisation in archaeological bones: the case study of Vicenne-Campochiaro necropolis (Italy). *J. Anal. Appl. Pyrolysis* 100, 173–180.
- Aldeias, V., Dibble, H.L., Sandgathe, D., Goldberg, P., McPherron, S.J.P., 2016. How heat alters underlying deposits and implications for archaeological fire features: a controlled experiment. *J. Archaeol. Sci.* 67, 64–79.
- Aldeias, V., Goldberg, P., Sandgathe, D., Berna, F., Dibble, H.L., McPherron, S.P., Turq, A., Rezek, Z., 2012. Evidence for Neandertal use of fire at Roc de Marsal (France). *J. Archaeol. Sci.* 39, 2414–2423.
- Behrensmeier, A., Kidwell, S., Gastaldo, R., 2000. Taphonomy and paleobiology. *Paleobiology* 26, 103–147.
- Berna, F., Goldberg, P., Horwitz, L.K., Brink, J., Holt, S., Bamford, M., Chazan, M., 2012. Microstratigraphic evidence of in situ fire in the Acheulean strata of Wonderwerk Cave, Northern Cape province, South Africa. *Proc. Natl. Acad. Sci.* 109, E1215–E1220.
- Bouchud, J., 1975. Etude de la faune de l'Abri Pataud, in: Movius, H.L.J. (Ed.), *Excavation of the Abri Pataud, Les Eyzies (Dordogne)*, Peabody Museum Press, Cambridge, pp. 69–153.
- Braadbaart, F., 2004. Carbonization of peas and wheat. A laboratory study. Leiden, The Netherlands. Available from: [www.amolf.nl](http://www.amolf.nl).
- Braadbaart, F., Boon, J.J., Veld, H., David, P., Van Bergen, P.F., 2004. Laboratory simulations of the transformation of peas as a result of heat treatment: changes of the physical and chemical properties. *J. Archaeol. Sci.* 31, 821–833.
- Braadbaart, F., Wright, P.J., van der Horst, J., Boon, J.J., 2007. A laboratory simulation of the carbonization of sunflower achenes and seeds. *J. Anal. Appl. Pyrolysis* 78, 316–327.
- Braadbaart, F., Poole, I., 2008. Morphological, chemical and physical changes during charcoalification of wood and its relevance to archaeological contexts. *J. Archaeol. Sci.* 35, 2434–2445.
- Braadbaart, F., Poole, I., van Brussel, A.A., 2009. Preservation potential of charcoal in alkaline environments: an experimental approach and implications for the archaeological record. *J. Archaeol. Sci.* 36, 1672–1679.
- Braadbaart, F., Poole, I., Huisman, D.J., et al., 2012. Fuel, Fire and Heat: An experimental approach to highlight the potential of studying ash and char remains from archaeological contexts. *J. Archaeol. Sci.* 39, 836–847.
- Braadbaart, F., Marinova, E., Sarpakai, A., 2016. Charred olive stones: experimental and archaeological evidence for recognizing olive processing residues used as fuel. *Veg. Hist. Archaeobot.* 25, 415–430.
- Briggs, A.W., Stenzel, U., Johnson, P.L., Green, R.E., Kelso, J., Prüfer, K., Meyer, M., Krause, J., Ronan, M.T., Lachmann, M., Pääbo, S., 2007. Patterns of damage in genomic DNA sequences from a Neandertal. *Proc Natl Acad Sci USA* 104 (37), 14616–14621.
- Brinkkemper, O., Braadbaart, F., van Os, B., van Hoesel, A., van Brussel, A.A.N., Fernandes, R., 2018. Effectiveness of different pre-treatments in recovering pre-burial isotopic ratios of charred plants. *Rapid Commun Mass Spectrom.* 32, 251–261.
- Brittingham, A., Hren, M.T., Hartman, G., Wilkinson, K.N., Mallol, C., Gasparyan, B., Adler, D.S., 2019. Geochemical Evidence for the Control of Fire by Middle Palaeolithic Hominins. *Sci. Rep.* 9, 15368.
- Brochier J.-E., Thimon M., 1993. Calcite crystals, starch grains aggregates or... POCC? Comment on 'calcite crystals inside archaeological plant tissues'. *Journal of Archaeological Science* 30(9) 2011–2124.
- Canti, M., Huisman, D.J., 2015. Scientific advances in geoarchaeology during the last twenty years. *J. Archaeol. Sci.* 56, 96–108.
- Carmody, R.N., Weintraub, G.S., Secor, S.M., Wrangham, R.W., 2010. Energetic significance of food processing: a test of the cooking hypothesis. *Integr. Comp. Biol.* 50, E24.
- Carmody, R.N., Weintraub, G.S., Wrangham, R.W., 2011. Energetic consequences of thermal and nonthermal food processing. *Proc. Natl. Acad. Sci.* 108, 19199–19203.
- Carmody, R.N., Wrangham, R.W., 2009. The energetic significance of cooking. *J. Hum. Evol.* 57, 379–391.
- Cersoy, S., Daheur, G., Zazzo, A., Zirah, S., Sablier, M., 2018. Pyrolysis comprehensive gas chromatography and mass spectrometry: A new tool to assess the purity of ancient collagen prior to radiocarbon dating. *Anal. Chim. Acta* 1041, 131–145.
- Chiavari, G., Galletti, G.C., 1992. Pyrolysis-gas chromatography/mass spectrometry of amino acids. *J. Anal. Appl. Pyrolysis* 24, 123–137.
- Chiotti, L., 2005. Les industries lithiques aurignaciennes de l'abri Pataud, Dordogne, France. Les fouilles de Hallam L. Movius Jr BAR International Series, Oxford.
- Cho, T.S., 1998. Etude archéozoologique de la faune du Périgordien supérieur : couches 2, 3 et 4 de l'abri Pataud, Les Eyzies, Dordogne : paléocécologie, taphonomie, paléocécologie, Muséum National d'Histoire Naturelle, Paris.
- Chowdhury, Z.Z., Karim, M.Z., Ashraf, M.A., Khalid, K., 2016. Influence of carbonization temperature on physicochemical properties of biochar derived from slow pyrolysis of durian wood (*Durio zibethinus*) sawdust. *BioResources* 11 (2), 3356–3372.
- Chrzavzez, J., Théry-Parisot, I., Fiorucci, G., Terral, J.F., Thibaut, B., 2014. Impact of post-depositional processes on charcoal fragmentation and archaeobotanical implications: experimental approach combining charcoal analysis and biomechanics. *Journal of Archeological Science* 44, 30–42.
- Cohen-Ofri, I., Weiner, L., Boaretto, E., Mintz, G., Weiner, S., 2006. Modern and fossil charcoal: aspects of structure and diagenesis. *J. Archaeol. Sci.* 33, 428–439.
- Collins, M., Nielsen-Marsh, C., Hiller, J., Smith, C., Prigodich, R., West, T., Csapo, J., Millard, A., Turner-Walker, G., 2002. The survival of organic matter in bone: a review. *Archaeometry* 3, 383–394.
- Collins, J.A., Carr, A.S., Schefuß, E., Boom, A., Sealy, J., 2017. Investigation of organic matter and biomarkers from Diepkloof Rock Shelter, South Africa: Insights into Middle Stone Age site usage and palaeoclimate. *J. Archaeol. Sci.* 85, 51–65.
- Costamagno, S., Théry-Parisot, I., Brugal, J.P., Guilbert, R., 2005. Taphonomic consequences of the use of bones as fuel: Experimental data and archaeological applications. In: O'Connor, T. (Ed.), *Biosphere to Lithosphere*. Oxbow, Oxford.
- Costamagno, S., Théry-Parisot, I., Kuntz, D., Bon, F., Mensan, R., 2010. Taphonomic impact of prolonged combustion on bones used as fuel, in: Théry-Parisot, I., Chabal, L., Costamagno, S. (Eds.), *The Taphonomy Of Burned Organic Residues And Combustion Features In Archaeological Contexts*. Proceedings of the round table, Valbonne, May 27–29, 2008. P@lethnologie, pp. 169–183.
- Crepin, L., 2013. Données archéozoologiques des grands mammifères, fouilles 2005-2008, in: Nespoulet, R., Chiotti, L., Henry-Gambier, D. (Eds.), *Le Gravettien final de l'abri Pataud (Les Eyzies, Dordogne. Résultats des fouilles et études 2005-2009*, Archaeopress (BAR International Series 2548), Oxford, pp. 63–88.
- Dibble, H.L., Sandgathe, D., Goldberg, P., McPherron, S., Aldeias, V., 2018. Were Western European Neandertals Able to Make Fire? *Journal of Paleolithic Archaeology* 1, 54–79.
- Douka, K., Nespoulet, R., Chiotti, L., Higham, T., 2020. A refined chronology for the Mid Upper Palaeolithic (Gravettian) sequence of Abri Pataud. *J. Hum. Evol.* 141, 102730.
- Emmons, H., Atreya, A., 1982. The science of wood combustion. *Proc. Indiana Acad. Sci.* 5, 259–268.
- Etiegni, L., Campbell, A., 1991. Physical and chemical characteristics of wood ash. *Bioresour. Technol.* 37, 173–178.
- Evans, E.J., Batts, B.D., Cant, N.W., Smith, J.W., 1985. The origin of nitriles in shale oils. *Org. Geochem.* 8, 367–374.
- Fabbri, D., Helleur, R.J., 1999. Characterization of the tetramethylammonium hydroxide thermochemical products of carbohydrates. *J. Anal. Appl. Pyrolysis* 49, 277–293.
- Fabbri, D., Torri, C., Spokas, K.A., 2012a. Analytical pyrolysis of synthetic chars derived from biomass with potential agronomic application (biochar). Relationships with impacts on microbial carbon dioxide production. *J. Anal. Appl. Pyrolysis* 93, 77–84.
- Fabbri, D., Adamiano, A., Falini, G., De Marco, R., Mancini, I., 2012b. Analytical pyrolysis of dipeptides containing proline and amino acids with polar side chains. Novel 2,5-diketopiperazine markers in the pyrolysates of proteins. *J. Anal. Appl. Pyrolysis* 95, 145–155.
- Fu, Q., Meyer, M., Gao, X., Stenzel, U., Burbano, H.A., Kelso, J., Pääbo, S., 2013. DNA analysis of an early modern human from Tianyuan Cave. *China. Proc Natl Acad Sci USA* 110 (6), 2223–2227.
- Gansauge, M.T., Gerber, T., Glocke, I., Korlević, P., Lippik, L., Nagel, S., Riehl, L.M., Schmidt, A., Meyer, M., 2017. Single-stranded DNA library preparation from highly

- degraded DNA using T4 DNA ligase. *Nucleic Acids Res.* 45 (10), e79.
- Glocke, I., Meyer, M., 2017. Extending the spectrum of DNA sequences retrieved from ancient bones and teeth. *Genome Res.* 27, 1230–1237.
- Günther, B., Gebauer, K., Barkowski, R., Rosenthal, M., Bues, C.T., 2012. Calorific value of selected wood species and wood products. *Eur. J. Wood Wood Prod.* 70, 755–757.
- Guo, Y., Bustin, R.M., 1998. FTIR spectroscopy and reflectance of modern charcoals and fungal decayed woods: implications for studies of inertinite in coals. *Int. J. Coal Geol.* 37, 29–53.
- Hartgers, W.A., Sinnighe Damsté, J.S., De Leeuw, J.W., 1995. Curie-point pyrolysis of sodium salts of functionalized fatty acids. *J. Anal. Appl. Pyrolysis* 34, 191–217.
- Hendrickler, A.D., Voorhees, K.J., 1998. Amino acid and oligopeptide analysis using Curie-point pyrolysis mass spectrometry with in-situ thermal hydrolysis and methylation: mechanistic considerations. *J. Anal. Appl. Pyrolysis* 48, 17–33.
- Henry, A., Théry-Parisot, I., 2014. From Evenk campfires to prehistoric hearths: charcoal analysis as a tool for identifying the use of rotted wood as fuel. *J. Archaeol. Sci.* 52, 321–336.
- Henry, A.G., Budel, T., Bazin, P.L., 2018. Towards an understanding of the costs of fire. *Quat. Int.* 493, 96–105.
- Higham, T., Jacobi, R., Basell, L., Ramsey, C.B., Chiotti, L., Nespoulet, R., 2011. Precision dating of the Palaeolithic: A new radiocarbon chronology for the Abri Pataud (France), a key Aurignacian sequence. *J. Hum. Evol.* 61, 549–563.
- Hlubik, S., Cutts, R., Braun, D.R., Berna, F., Feibel, C.S., Harris, J.W.K., 2019. Hominin fire use in the Okote member at Koobi Fora, Kenya: New evidence for the old debate. *J. Hum. Evol.* 133, 214–229.
- Hoesel van, A., Reidsma, F.H., Os van, B.J.H., Megens, L., Braadbaart, F., 2019. Combusted bone: Physical and chemical changes of bone during laboratory simulated heating under oxidising conditions and their relevance for the study of ancient fire use. *J. Archaeol. Sci.: Rep.* 28, 102033.
- Huson, D.H., Auch, A.F., Qi, J., Schuster, S.C., 2007. MEGAN analysis of metagenomic data. *Genome Res.* 17 (3), 377–386.
- ISO 7404-2, 1985. International Standard. Methods for the Petrographic Analysis of Bituminous Coal and Anthracite – Part 2: Method of Preparing Coal Samples. Ref. No. ISO 7404/2-1985 (E).
- ISO 7404-5, 1994. International Standard. Methods for the Petrographic Analysis of Bituminous Coal and Anthracite – Part 5: Method of Determining Microscopically the Reflectance of Vitrinite. Ref. No. ISO 7404-5: 1994 (E).
- Kaal, J., Martínez-Cortizas, A., Nierop, K.G.J., Buurman, P., 2008. A detailed pyrolysis-GC/MS analysis of a black carbon-rich acidic colluvial soil (Atlantic ranker) from NW Spain. *Appl. Geochem.* 23, 2395–2405.
- Kaal, J., Martínez, Cortizas A., Reyes, O., Soliño, M., 2012. Molecular characterization of *Ulex europaeus* biochar obtained from laboratory heat treatment experiments—a pyrolysis-GC/MS study. *J. Anal. Appl. Pyrolysis* 95, 205–212.
- Kaal, J., Filley, T.R., 2016. Novel molecular proxies for inferring pyrogenic black carbon oxidation state using thermally assisted hydrolysis and methylation (THM-GC-MS) with <sup>13</sup>C-labeled tetramethylammonium hydroxide (TMAH). *J. Anal. Appl. Pyrolysis* 121, 146–154.
- Kaal, J., López-Costas, O., Cortizas, Martínez, 2016. Diagenetic effects on pyrolysis fingerprints of extracted collagen in archaeological human bones from NW Spain, as determined by pyrolysis-GC-MS. *J. Archaeol. Sci.* 65, 1–10.
- Kaal, J., Linderholm, J., Martínez Cortizas, A., 2019. Fire, meat and totarol: organic matter in the embankments of the Neolithic site Bastuloken (North Sweden). *Analytical Pyrolysis Letters APL007*. [www.pyrolysis.com/apl007](http://www.pyrolysis.com/apl007).
- Karkanias, P., Bar-Yosef, O., Goldberg, P., Weiner, S., 2000. Diagenesis in Prehistoric Caves: the Use of Minerals that Form In Situ to Assess the Completeness of the Archaeological Record. *J. Archaeol. Sci.* 27, 915–929.
- Kedrowski, B.L., Crass, B.A., Behm, J.A., Luetke, J.C., Nichols, A.L., Moreck, A.M., Holmes, C.E., 2009. GC/MS Analysis of Fatty Acids from Ancient Hearth Residues at the Swan Point Archaeological Site. *Archaeometry* 51, 110–122.
- Kircher, M., Sawyer, S., Meyer, M., 2012. Double indexing overcomes inaccuracies in multiplex sequencing on the Illumina platform. *Nucleic Acids Res.* 40 (1), e3.
- Klein, A., Krebs, O., Gehl, A., Morgner, J., Reeger, L., Augustin, C., Edler, C., 2018. Detection of blood and DNA traces after thermal exposure. *Int. J. Legal Med.* 132, 1025–1033.
- Knicker, H., del Río, J.C., Hatcher, P.G., Minard, R.D., 2001. Identification of protein remnants in insoluble geopolymers using TMAH thermochemistry/GC-MS. *Org. Geochem.* 32, 397–409.
- Lejay, M., Alexis, M., Quénéa, K., Sellami, F., Bon, F., 2016. Organic signatures of fireplaces: Experimental references for archaeological interpretations. *Org. Geochem.* 99, 67–77.
- Lejay, M., Alexis, M.A., Quénéa, K., Anquetil, C., Bon, F., 2019. The organic signature of an experimental meat-cooking fireplace: The identification of nitrogen compounds and their archaeological potential. *Org. Geochem.* 138, 103923.
- Lenoble, A., Agsous, S., 2012. Abri Pataud – sédimentogénèse, paléopédologie, chronologie des dépôts. , in: Bertran, P., Lenoble, A. (Eds.), *Quaternaire continental d'Aquitaine :Un point sur les travaux récents*. Livret-Guide Excursion AFEQ – ASF en Aquitaine, 30 mai - 1 juin 2012. INRAP/Grand Sud Ouest, Bordeaux, pp. 45-57.
- Liu, C., Hu, J., Zhang, H., Xiao, R., 2016. Thermal conversion of lignin to phenols: Relevance between chemical structure and pyrolysis behaviors. *Fuel* 182, 864–870.
- Lyman, R.L., 1994. *Vertebrate Taphonomy*. Cambridge University Press, Cambridge.
- Marčić, T., Whitten, M., Pääbo, S., 2010. Multiplexed DNA sequence capture of mitochondrial genomes using PCR products. *PLoS ONE* 5 (11), e14004.
- Marquer, L., 2010. From microcharcoal to macrocharcoal: reconstruction of the “wood charcoal” signature in Palaeolithic archaeological contexts. *Palaeol. 2*, 105–115.
- Marquer, L., Otto, T., Nespoulet, R., Chiotti, L., 2010. A new approach to study the fuel used in hearths by hunter-gatherers at the Upper Palaeolithic site of Abri Pataud (Dordogne, France). *J. Archaeol. Sci.* 2735–2746.
- Marquer, L., Lebreton, V., Otto, T., Valladas, H., Haesaerts, P., Messenger, E., Nuzhnyi, D., Péan, S., 2012. Charcoal scarcity in Epigravettian settlements with mammoth bone dwellings: the taphonomic evidence from Mezhyrich (Ukraine). *J. Archaeol. Sci.* 39, 109–120.
- Marquer, L., Lebreton, V., Otto, T., Messenger, E., 2015. Étude des macro-, méso- et micro-charbons du site épigravettien de Mezhyrich (Ukraine): données taphonomiques et anthracologiques. *L'Anthropologie* 119, 487–504.
- McCauley, B., Collard, M., Sandgathe, D., 2020. In press. A Cross-cultural Survey of On-site Fire Use by Recent Hunter-gatherers: Implications for Research on Palaeolithic Pyrotechnology. *Journal of Paleolithic Archaeology*.
- Meyer, M., Arsuaga, J.L., de Filippo, C., Nagel, S., Aximu-Petri, A., Nickel, B., Martínez, I., Gracia, A., Bermúdez de Castro, J.M., Carbonell, E., Viola, B., Kelso, J., Prüfer, K., Pääbo, S., 2016. Nuclear DNA sequences from the Middle Pleistocene Sima de los Huesos hominins. *Nature* 531 (7595), 504–507.
- Miller, C.E., Conard, N.J., Goldberg, P., Berna, F., 2009. Dumping, sweeping and trampling: Experimental micromorphological analysis of anthropogenically modified combustion features, in: Thery-Parisot, I., Chabal, L., Costamagno, S. (Eds.), *The Taphonomy of Burned Organic Residues and Combustion Features in Archaeological Contexts*. Proceedings of the round table, Valbonne, May 27-29 2008. *Paleoethnology* 2, 25–37.
- Movius, H.L.Jr., 1965a. Upper Perigordian and Aurignacian Hearths at the Abri Pataud, Les Eyzies (Dordogne), Miscelana En Homenaje al Abate Henri Breuil, Instituto de Prehistoria Y Arqueologia, Barcelona, pp. 182-196.
- Movius H.L.Jr., 1965b. Aurignacian Hearths at the Abri Pataud Les Eyzies (Dordogne), Symposium in Honor of Dr. Li Chi on his Seventieth Birthday, Institute of History and Philology, Academia Sinica, Taipei, Taiwan, pp. 303-316.
- Movius Jr., H.L., 1966. The Hearths of the Upper Périgordian and Aurignacian Horizons at the Abri Pataud, Les Eyzies (Dordogne), and Their Possible Significance. *American Anthropologist* 68, 296–325.
- Movius H.L. Jr. 1975. – Excavation of the abri Pataud, Les Eyzies (Dordogne): Contributors, American School of Prehistoric Research, 30, Peabody Museum, Harvard University, Cambridge, Massachusetts, 305 p.
- Movius H.L. Jr 1977. Excavation of the Abri Pataud, Les Eyzies (Dordogne): Stratigraphy. American School of Prehistoric Research, 31. Cambridge: Peabody Museum, Harvard University. 167 p.
- Munro, L.E., Longstaffe, F.J., White, C.D., 2007. Burning and boiling of modern deer bone: effects on crystallinity and oxygen isotope composition of bioapatite phosphate. *Palaeogeogr. Palaeoclimatol. Palaeoecol.* 249, 90–102.
- Nespoulet, R., Chiotti, L., 2007. 1953-2004: La Collection Movius de l'abri Pataud (les Eyzies-de-Tayac, Dordogne) Conference Paper.
- Nespoulet, R., 2008. Le Gravettien de l'abri Pataud, bilan et perspectives. *Paléo* 20, 373–380.
- Nguyen, M.N., Dultz, S., Guggenberger, G., 2014. Effects of pretreatment and solution chemistry on solubility of rice-straw phytoliths. *J. Plant Nutr. Soil Sci.* 177, 349–359.
- Nierop, K.G.J., Van Bergen, P.F., 2002. Clay and ammonium catalyzed reactions of alkanols, alkanolic acids and esters under flash pyrolytic conditions. *J. Anal. Appl. Pyrolysis* 63, 197–208.
- Nishimiya, K., Hata, T., Imamura, Y., Ishihara, S., 1998. Analysis of chemical structure of wood charcoal by X-ray photoelectron spectroscopy. *Journal of Wood Science* 44, 56–61.
- Orsini, S., Parlanti, F., Bonaduce, I., 2017. Analytical pyrolysis of proteins in samples from artistic and archaeological objects. *J. Anal. Appl. Pyrolysis* 124, 643–657.
- Oudemans, T.F.M., Boon, J.J., Botto, R.E., 2007. FTIR and solid-state <sup>13</sup>C CP/MAS NMR spectroscopy of charred and non-charred solid organic residues preserved in Roman Iron Age vessels from the Netherlands. *Archaeometry* 49 (3), 271–294.
- Person, A., Bocherens, H., Saliège, J.-F., Paris, F., Zeitung, V., Gerard, M., 1995. Early diagenetic evolution of bone phosphate: an X-ray diffractometry analysis. *Journal of Archaeological Science* 22, 211–221.
- Pestle, W.J., 2010. Chemical, elemental, and isotopic effects of acid concentration and treatment duration on ancient bone collagen: an exploratory study. *Journal of Archaeological Science* 37, 3124–3128.
- Reidsma, F.H., van Hoesel, A., van Os, B.J.H., Megens, L., Braadbaart, F., 2016. Charred bone: Physical and chemical changes during laboratory simulated heating under reducing conditions and its relevance for the study of fire use in archaeology. *J. Archaeol. Sci.: Rep.* 10, 282–292.
- Rein, G., 2009. Smouldering Combustion Phenomena in Science and Technology. *Int. Rev. Chem. Eng.* 1, 3–18.
- Roebroeks, W., Villa, P., 2011. On the earliest evidence for habitual use of fire in Europe. *Proc. Natl. Acad. Sci.* 108, 5209–5214.
- Rohland, N., Glocke, I., Aximu-Petri, A., Meyer, M., 2018. Extraction of highly degraded DNA from ancient bones, teeth and sediments for high-throughput sequencing. *Nat. Protoc.* 13, 2447–2461.
- Sawyer, S., Krause, J., Guschanski, K., Savolainen, V., Pääbo, S., 2012. Temporal Patterns of Nucleotide Mismatches and DNA Fragmentation in Ancient DNA. *PLoS ONE* 7 (3), e34131.
- Scherjon, F., Bakels, C., MacDonald, K., Roebroeks, W., 2015. Burning the Land: An Ethnographic Study of Off-Site Fire Use by Current and Historically Documented Foragers and Implications for the Interpretation of Past Fire Practices in the Landscape. *Current Anthropology* 56, 299–326.
- Sekhr, A., 1998. Etude archéozoologique des niveaux aurignaciens (couches 14 à 6) et de la base des niveaux gravettiens (niveaux X à T4) de l'abri Pataud (Les Eyzies, Dordogne). *Paléocécologie, taphonomie, paléontologie Muséum National d'Histoire Naturelle*, Paris.
- Shafizadeh, F., 1975. Industrial pyrolysis of cellulosic materials. *Appl. Polym. Symp.* 28, 153–174.
- Shimelmitz, R., Kuhn, S.L., Jelinek, A.J., Ronen, A., Clark, A.E., Weinstein-Evron, M.,

2014. 'Fire at will': The emergence of habitual fire use 350,000 years ago. *J. Hum. Evol.* 77, 196–203.
- Slon, V., Glocke, I., Barkai, R., Gopher, A., Hershkovitz, I., Meyer, M., 2016. Mammalian mitochondrial capture, a tool for rapid screening of DNA preservation in faunal and undiagnostic remains, and its application to Middle Pleistocene specimens from Qesem Cave (Israel). *Quat. Int.* 398, 210–218.
- Slon, V., Hopfe, C., Weiß, C.L., Mafessoni, F., de la Rasilla, M., Laluzza-Fox, C., Rosas, A., Soressi, M., Knul, M.V., Miller, R., Stewart, J.R., Derevianko, A.P., Jacobs, Z., Li, B., Roberts, R.G., Shunkov, M.V., de Lumley, H., Perrenoud, C., Gušić, I., Kučan, Ž., Rudan, P., Aximu-Petri, A., Essel, E., Nagel, S., Nickel, B., Schmidt, A., Prüfer, K., Kelso, J., Burbano, H.A., Pääbo, S., Meyer, M., 2017. Neandertal and Denisovan DNA from Pleistocene sediments. *Science* 356 (6338), 605–608.
- Smith, A., Proctor, L., Hart, T.C., Stein, G.J., 2019. The burning issue of dung in archaeobotanical samples: a case-study integrating macro-botanical remains, dung spherulites, and phytoliths to assess sample origin and fuel use at Tell Zeidan. *Syria, Vegetation History and Archaeobotany* 28, 229–246.
- Sorensen, A., Roebroeks, W., van Gijn, A., 2014. Fire production in the deep past? The expedient strike-a-light model. *J. Archaeol. Sci.* 42, 476–486.
- Speth, J.D. 2010. *The Paleoanthropology and Archaeology of Big-Game Hunting. Protein, fat or politics?* New York: Springer.
- Théry-Parisot, I., 2002. Fuel Management (Bone and Wood) During the Lower Aurignacian in the Pataud Rock Shelter (Lower Palaeolithic, Les Eyzies de Tayac, Dordogne, France). *Contribution of Experimentation. J. Archaeol. Sci.* 29, 1415–1421.
- Théry-Parisot, I., Costamagno, S., 2005. Propriétés combustibles des ossements : données expérimentales et réflexions archéologiques sur leur emploi dans les sites paléolithiques. *Gallia Préhistoire* 235–254.
- Théry-Parisot, I., Costamagno, S., Brugal, J.-P., Fosse, P., Guilbert, R., 2005. The use of bone as fuel during the Palaeolithic, experimental study of bone combustible properties, in: Mulville, J., Outram, A.K. (Eds.), *The Zooarchaeology of Fats, Oils, Milk and Dairying. Proceedings of the 9th ICAZ Conferences (Durham, August 2002)*. Oxbow Books, Durham, pp. 50–59.
- Théry-Parisot, I., Costamagno, S., Henry, A., 2009. Gestion des combustibles au paléolithique et au mésolithique: Nouveaux outils, nouvelles interprétations, in: Oosterbeek, L. (Ed.), *BAR International Series. Archaeopress, Oxford*.
- Théry-Parisot, I., Chabal, L., Chravzez, J., 2010. Anthracology and taphonomy, from wood gathering to charcoal analysis. A review of the taphonomic processes modifying charcoal assemblages, in archaeological contexts. *Palaeogeogr. Palaeoclimatol. Palaeoecol.* 291, 142–153.
- Théry-Parisot, I., Henry, A., 2012. Seasoned or green? Radial cracks analysis as a method for identifying the use of green wood as fuel in archaeological charcoal. *J. Archaeol. Sci.* 39, 381–388.
- Théry-Parisot, I., Thiebault, S., Delannoy, J.J., Ferrier, C., Feruglio, V., Fritz, C., Gely, B., Guibert, P., Monney, J., Tosello, G., Clottes, J., Geneste, J.-J., 2018. Illuminating the cave, drawing with black wood charcoal: new insights from la grotte Chauvet (Vallon-Pont d'Arc, France) through charcoal fragments analysis. *Antiquity* 92, 320–333.
- Ulery AL, Drees RD 2008. *Methods of Soil Analysis part 5—Mineralogical Methods*. In :Soil Science Society of America Book Series. Published by Soil Science Society of America, Inc., Madison, Wisconsin, USA.
- Vaiglova, P., Snoeck, C., Nitsch, E., Bogaard, A., Lee-Thorp, J., 2014. Impact of contamination and pre-treatment on stable carbon and nitrogen isotopic composition of charred plant remains. *Rapid Commun Mass Spectrom.* 28 (23), 2497–2510.
- Vannoorenberghe, A., 2004. *Contribution à la connaissance des comportements de subsistance des gravettien du sud-ouest de la France. La faune du Gravettien ancien de l'abri Pataud (Les Eyzies-de-Tayac, Dordogne)*, Muséum National d'Histoire Naturelle, Paris.
- Vidal-Matutano, P., Henry, A., Théry-Parisot, I., 2017. Dead wood gathering among Neanderthal groups: charcoal evidence from Abric del Pastor and El Salt (eastern Iberia). *J. Archaeol. Sci.* 80, 109–121.
- Villa, P., Bon, F., Castel, J.-C., 2002. Fuel, Fire and Fireplaces in the Palaeolithic of Western Europe. *The Review of Archaeology* 23 (1), 33–42.
- Weiner, S., Bar-Yosef, O., 1990. States of preservation of bones from prehistoric sites in the Near East: a survey. *J. Archaeol. Sci.* 17, 187–196.
- Weiner, S., 2010. *Microarchaeology: Beyond the visible archaeological record*. Cambridge University Press, Cambridge.
- White, R., Mensan, R., Clark, A.E., Tartar, E., Marquer, L., Bourrillon, R., Goldberg, P., Chiotti, L., Cretin, C., Rendu, W., 2017. Technologies for the control of heat and light in the Vézère Valley Aurignacian. *Current Anthropology* 58, S288–S302.
- Wiessner, P., 2014. Embers of society: Firelight talk among the Ju/'hoansi Bushmen. *Proc. Natl. Acad. Sci.* 111, 14027–14035.
- Wrangham, R., 2009. *Catching fire: How cooking made us human*. Basic Books, New York.
- Wrangham, R., 2013. The evolution of human nutrition. *Curr. Biol.* 23, R354–R355.
- Wroth, K., Cabanes, D., Marston, J.M., Aldeias, V., Sandgathe, D., Turq, A., Goldberg, P., Dibble, H.L., 2019. Neanderthal plant use and pyrotechnology: phytolith analysis from Roc de Marsal. *France, Archaeological and Anthropological Sciences* 11, 4325–4346.
- Xiao, B., Sun, X., Sun, R., 2001. Chemical, structural, and thermal characterizations of alkali-soluble lignins and hemicelluloses, and cellulose from maize stems, rye straw, and rice straw. *Polym. Degrad. Stab.* 74, 307–319.
- Zgusta, R., 2015. *The peoples of northeast Asia through time: precolonial ethnic and cultural processes along the coast between Hokkaido and the Bering Strait*, Brill, Leiden/Boston.